bioRxiv preprint doi: https://doi.org/10.1101/2023.03.22.533738; this version posted March 24, 2023. The copyright holder for this preprint (which was not certified by peer review) is the author/funder, who has granted bioRxiv a license to display the preprint in perpetuity. It is made available under aCC-BY-NC-ND 4.0 International license.

The new signaling pathway ERK5/TP53INP2 sensitizes cancer cells to death-receptor agonists and Natural Killer cells

Sergio Espinosa-Gil[1,2], Saska Ivanova[3], Elisenda Alari-Pahissa[4], Melek Denizli[5]; Beatriz Villafranca-Magdalena[5], Maria Viñas-Casas[1,2], Idoia Bolinaga-Ayala[1,2], Andrés Gámez-García[1], Eva Colas[5], Miguel Lopez-Botet[4,6], Antonio Zorzano[3,7], José Miguel Lizcano[1,2]

1. Departament de Bioquímica i Biologia Molecular and Institut de Neurociències. Facultat de Medicina, Universitat Autònoma de Barcelona (UAB), Barcelona, Spain.

2. Protein Kinases in Cancer Research. Vall d'Hebron Institut de Recerca (VHIR), Barcelona, Spain.

3. IRB Institute for Research in Biomedicine, Barcelona, Spain. CIBERDEM, Instituto de Salud Carlos III, Spain.

4. University Pompeu Fabra, Barcelona, Spain

5. Biomedical Research Group in Gynecology, Vall Hebron Institute of Research, Universitat Autònoma de Barcelona. CIBERONC, Barcelona, Spain.

6. Immunology laboratory, Dpt. of Pathology. Hospital del Mar Medical Research Institute (IMIM), Barcelona, Spain

7. Departament de Bioquímica i Biomedicina Molecular, Facultat de Biología. Universitat de Barcelona, Spain.

Corresponding author and address:

Jose M Lizcano,

Vall Hebron Institut de Recerca (VHIR), Edifici Collserola

Laboratory 143, Protein Kinases in Cancer Research.

Passeig de la Vall d'Hebron, 119-129

08035 Barcelona, SPAIN

Phone: +34 935 274 6739

Email: josemiguel.lizcano@uab.es; Jose.lizcano@vhir.org

bioRxiv preprint doi: https://doi.org/10.1101/2023.03.22.533738; this version posted March 24, 2023. The copyright holder for this preprint (which was not certified by peer review) is the author/funder, who has granted bioRxiv a license to display the preprint in perpetuity. It is made available under aCC-BY-NC-ND 4.0 International license.

Abstract 150 words

The extrinsic apoptotic pathway is initiated by the binding of TRAIL, TNFα or FasL to their cognate death receptors (DRs), leading to the intracellular assembly of the DISC complex and activation of caspase-8. Here, using 2D and 3D cell cultures and patient-derived xenograft organoids, we described a new signaling pathway that regulates activation of caspase-8 in response to DR agonists in cancer cells. Mechanistically, ERK5 phosphorylates and induces ubiquitylation and proteasomal degradation of TP53INP2, a protein that mediates caspase-8 activation in response to DR agonists. Concordantly, ERK5 inhibition or genetic deletion induced TP53INP2 protein stabilization and sensitized cancer cells to DR agonists-induced extrinsic apoptosis, whereas ERK5 kinase activity protected cancer cells from apoptosis induced by DR agonists. Since TRAIL selectively induces apoptosis in cancer cells, our results support the use of ERK5 inhibitors as an effective strategy to sensitize cancer cells to TRAIL-based therapies, including Natural Killer cells expressing TRAIL.

bioRxiv preprint doi: https://doi.org/10.1101/2023.03.22.533738; this version posted March 24, 2023. The copyright holder for this preprint (which was not certified by peer review) is the author/funder, who has granted bioRxiv a license to display the preprint in perpetuity. It is made available under aCC-BY-NC-ND 4.0 International license.

bioRxiv preprint doi: https://doi.org/10.1101/2023.03.22.533738; this version posted March 24, 2023. The copyright holder for this preprint (which was not certified by peer review) is the author/funder, who has granted bioRxiv a license to display the preprint in perpetuity. It is made available under aCC-BY-NC-ND 4.0 International license.

Introduction.

Apoptosis, a programmed cell death process, can be triggered through either the intrinsic or the extrinsic pathways. The intrinsic apoptotic pathway is activated in response to intracellular stimuli that induce cellular damage. Briefly, in response to cellular damage apoptotic sensors of the Bcl-2 family induce mitochondrial outer membrane permeabilization (MOMP), which leads to cytochrome c release into the cytosol, promoting the formation of the apoptosome[1]. Apoptosome formation drives caspase-9 activation, which in turn cleaves and activates the executor caspases -3, -6 and -7[2]. Extrinsic apoptosis is induced by direct interaction of so-called death ligands (TNFα, FasL and TNF-related apoptosis-inducing ligand TRAIL) with their specific death-receptors (DRs) at the plasma membrane. Death ligand binding induces the trimerization of the DR, triggering the formation of the so-called death-inducing signaling complex (DISC) comprising FADD and several molecules of pro-caspase-8[3]. FADD acts as an adaptor protein that allows the orientation and dimerization of pro-caspase-8 molecules, allowing the activation of caspase-8 by proximity-induced proteolytic cleavage[4, 5]. Then, in type-I cells, active caspase-8 cleaves and directly activates executioner caspase-3, thereby inducing cellular apoptosis. In contrast, in type-II cells (which mainly rely on intrinsic apoptosis), active caspase-8 cleaves Bid into truncated Bid (tBid), which promotes signal amplification by inducing mitochondrial outer membrane permeabilization[6, 7]. Several studies have underlined caspase-8 ubiquitylation as a critical process for caspase-8 activation. Thus, TRAF2-mediated caspase-8 K48-ubiquitylation promotes proteasomal degradation of caspase-8, limiting DISC activity[8]. In contrast, caspase-8 K63-ubiquitylation by Cullin3 or TRAF6 ligases promotes the aggregation, self-processing and full activation of caspase-8[9, 10]. However, efficient K63-ubiquitylation of caspase 8 requires of other players that facilitate the recruitment of the ligases to the DISC complex. For example, in response to DRs activation, TP53INP2 binds caspase-8 and the TRAF6-Ubc13 dimer, allowing a more efficient ubiquitin transfer from Ubc13 to caspase-8[11].

Among DR ligands, TRAIL triggers extrinsic apoptotic cell death through TRAIL receptors DR4 and DR5. Importantly, TRAIL induces apoptosis in a wide variety of cancer cell lines and tumors, without affecting normal cells[12]. Therefore, TRAIL-receptor agonists (TRAs) have been extensively investigated as promising cancer therapies, and are currently in clinical trials for several solid cancers, including NSCLC, multiple myeloma and advanced hepatocellular carcinoma[13]. However, despite promising preclinical observations, TRAIL–based therapies in humans have shown limitations, mainly due to their poor ability

bioRxiv preprint doi: https://doi.org/10.1101/2023.03.22.533738; this version posted March 24, 2023. The copyright holder for this preprint (which was not certified by peer review) is the author/funder, who has granted bioRxiv a license to display the preprint in perpetuity. It is made available under aCC-BY-NC-ND 4.0 International license.

to activate caspase-8 in solid tumors (reviewed in[13]). Hence, to improve TRAIL-based anticancer therapy, it is critical to identify those cellular pathways involved in the sensitization to TRAIL-induced apoptosis.

The MAPK extracellular regulated kinase 5 (ERK5) is activated in response to growth factors and different forms of stress, including oxidative stress and cytokines[14]. ERK5 is activated by direct phosphorylation of its unique upstream kinase MEK5[15]. The MEK5-ERK5 pathway constitutes a unique intracellular axis that mediates cell proliferation and survival of several cancer paradigms, including blood and solid cancers[16, 17]. Furthermore, it has been shown that high levels of ERK5 or MEK5 correlate with bad prognosis and malignancy of several cancers, including hepatocellular carcinoma, breast, endometrial and prostate cancers[18-21]. In addition, ERK5 kinase activity protects cancer cells from entering apoptosis. Among others, ERK5 phosphorylates and inhibits Bad and Bim pro-apoptotic proteins, impairing intrinsic apoptosis in proliferating cells[22, 23]. According to these observations, ERK5 has been proposed as a new target to tackle different solid cancers, and ERK5 inhibitors have shown anticancer activity in tumor xenograft models[24].

In this study, we have investigated the role of the MEK5-ERK5 pathway in the extrinsic apoptosis induced by DR agonists in cancer cells. We found that ERK5 kinase activity confers resistance to the cytotoxicity exerted by DR agonists in cancer cells, by phosphorylating and inducing proteasomal degradation of TP53INP2, a protein required to achieve full caspase-8 activation. Concordantly, pharmacologic or genetic ERK5 inhibition sensitized cancer cells to apoptosis induced by DR agonists and by TRAIL/FasL expressed by NK cells.

bioRxiv preprint doi: https://doi.org/10.1101/2023.03.22.533738; this version posted March 24, 2023. The copyright holder for this preprint (which was not certified by peer review) is the author/funder, who has granted bioRxiv a license to display the preprint in perpetuity. It is made available under aCC-BY-NC-ND 4.0 International license.

Results

ERK5 kinase activity modulates sensitivity of cancer cell to DR agonists.

There is much interest in using death receptor (DR) agonists in cancer treatment. Among DR agonists, TRAIL-based therapies are currently in clinical trials to treat solid cancers, since TRAIL selectively induces apoptosis in cancer cells[12]. However, many primary tumors show inherent resistance to TRAIL-induced apoptosis. Therefore, current efforts are focussed on dissecting the intracellular signaling pathways involved in resistance to TRAIL, to identify strategies that sensitize cancer cells to TRAIL-induced cytotoxicity. A RNAi-based screening identified ERK5 as one of top 5% genes whose silencing sensitized HeLa cells to TRAIL-induced apoptosis[25]. In this regard, following studies reported that overexpression of a constitutive nuclear ERK5 mutant favored resistance to TRAIL-induced apoptosis in breast cancer cells[26]. These preliminary works prompted us to investigate whether ERK5 pathway is implicated in resistance to TRAIL-induced toxicity in cancer cells.

To investigate the role of ERK5 as a modulator of extrinsic apoptosis induced by DR agonists, we used endometrial cancer (EC) cells. EC cells frequently show overactivation of PI3K/mTOR (~50% of EC cells harbour a double allelic mutated PTEN gene) and canonical NF-kB pathways, which protect cancer cells from TRAIL-induced apoptosis[27, 28]. Thus, EC cells represent a good model of TRAIL-resistant cancer cells. We recently showed that ERK5 inhibition or silencing impaired NF-kB transcriptional activity and induced apoptosis in a panel of EC cells carrying *PTEN* deletion or inactivating mutations[20]. Here, we first investigated the effect of ERK5 inhibition in TRAIL-induced cytotoxicity. We tested the effect of the specific ERK5 inhibitor JWG-071[20, 29] in a panel of human EC cell lines, including type I endometroid (Ishikawa and ANC3A) and type II non-endometroid (ARK1 and ARK2) cells. Cell viability assays showed that pre-treatment with JWG-071 (12h) sensitized the four EC cell lines to recombinant TRAIL (rTRAIL)-induced cytotoxicity in a dose-dependent manner (**Fig. 1A)**. To discard an off-target effect of the JWG-071 compound, we also tested the structurally different ERK5 inhibitor AX15836[30] as well as the MEK5 inhibitors BIX02188 and BIX02189[31]. As shown in **Fig. 1B**, all the inhibitors of the MEK5-ERK5 pathway sensitized EC cells to TRAIL-induced cell death. Interestingly, ERK5 inhibition also sensitized EC cells to the toxicity induced by other DR ligands such as TNFα or FasL (**Fig. 1C**), indicating a role for ERK5 kinase activity in mediating the extrinsic apoptosis induced by DR agonists in cancer cells. Finally, we also tested the effect of ERK5 inhibition in cell lines derived from other human cancer types that were reported to be resistant to TRAIL, such as neuroblastoma (SK-N-AS), cervical

bioRxiv preprint doi: https://doi.org/10.1101/2023.03.22.533738; this version posted March 24, 2023. The copyright holder for this preprint (which was not certified by peer review) is the author/funder, who has granted bioRxiv a license to display the preprint in perpetuity. It is made available under aCC-BY-NC-ND 4.0 International license.

(HeLa), non-small cell lung (A549), and prostate (LnCaP) cancer cells[32-35]. The ERK5 inhibitor potentiated TRAIL cytotoxicity in all cancer cell lines tested (**Fig. 1D)**, suggesting that ERK5 inhibition sensitizes cancer cells to TRAIL, independently of cancer type or mutational status.

Of note, Ishikawa cells exhibited the highest resistance to TRAIL (IC_{50} > 150 ng/ml), and therefore they represent a good model to dissect the mechanism by which ERK5 inhibitors improve TRAIL anticancer activity. Since caspase-8 plays a central role in the extrinsic apoptotic pathway in response to DR ligands[36], we first monitored the activation of caspase-8 and the effector caspase-3 by immunoblot analysis. As observed in **Fig. 1E,** ERK5 inhibition (ERK5i) potentiated the activation of caspase-8 (and activation of its substrate caspase-3) in response to rTRAIL, TNFα or anti-Fas activating antibody, but it had no effect when incubated alone. In addition, preincubation with the pan-caspase inhibitor QVD-OPh mostly reverted the cytotoxicity induced by the combined TRAIL and JWG-071 treatment **(Fig. 1F**), demonstrating a role of caspases in ERK5i-mediated sensitization to TRAIL.

The aforementioned results suggest that ERK5 kinase activity protects cancer cells from apoptosis induced by DR ligands. To test this hypothesis, we investigated the impact of the MEK5-ERK5 pathway activity in the apoptosis induced by TRAIL. For this purpose, we used the AN3CA EC cell line, which was the most sensitive to TRAIL-induced apoptosis (IC_{50}, 25 ng/ml). We transiently overexpressed either wild type ERK5 or the ERK5 kinase-dead mutant (ERK5-KD, in which the Asp^{200} residue of the catalytic loop was mutated to Ala), in combination with a constitutive active form of MEK5 (MEK5-DD, in which residues Ser^{311} and Ser^{315} were mutated to Asp). Flow cytometry analysis (Anexin-V/PI) showed that overexpression of active ERK5, but not of kinase dead ERK5, resulted in a significant lower number of apoptotic cells in response to TRAIL treatment, as measured by Annexin V staining and caspase-8 activation assays **(Fig. 2A-B).** Similar results were obtained in Ishikawa EC cells (**Fig. 2C**). Thus, ERK5 kinase activity protects cells from TRAIL-induced apoptosis.

To obtain genetic evidences on the role of ERK5 activity in sensitization to TRAIL-induced apoptosis, we used CRISPR/Cas9 technology to generate stable Ishikawa cell lines where MEK5 or ERK5 genes were genetically deleted. MEK5 is the only kinase that activates ERK5 by direct phosphorylation of the TEY motif, and ERK5 is the only known substrate described for MEK5[37]. Therefore, MEK5 knockout cells lack ERK5 kinase activity. We recently reported that MEK5-KO Ishikawa cells, while lacking ERK5 activity, show normal activation of other MAP kinases (ERK1/2, p38s or JNKs), or components of the PI3K pathway (Akt, mTORC1 or p70S6K) in response to mitogens, stressors or insulin[20]. On the other

bioRxiv preprint doi: https://doi.org/10.1101/2023.03.22.533738; this version posted March 24, 2023. The copyright holder for this preprint (which was not certified by peer review) is the author/funder, who has granted bioRxiv a license to display the preprint in perpetuity. It is made available under aCC-BY-NC-ND 4.0 International license.

hand, ERK5-KO cells lack both kinase activity-dependent and -independent functions. MEK5 or ERK5 genetic deletion sensitized Ishikawa cells to the apoptosis induced by DR agonists TRAIL, TNFα and anti-Fas activating antibody, as measured by Annexin-V binding and caspase-8 and -3 activation (**Fig. 3A-C**). Similar results were obtained in cervical HeLa and NSCLC A549 MEK5-KO cells, where TRAIL induced higher cytotoxicity compared to wild type cells (**Suppl. Fig. 1**). As seen for the ERK5 inhibitor, ERK5-KO and MEK5-KO Ishikawa cells also showed enhance caspase-8 and -3 activation in response to DR ligands **(Fig. 3B and 3C**, respectively). Finally, we tested the cytotoxic effect of DR agonists in 3D cultures of MEK5 wild type or KO Ishikawa cells, a more complex model to test the effect of drugs. In LIVE/DEAD fluorescence staining assays, 3D cultures of cells lacking ERK5 kinase activity (MEK5-KO cells) showed higher sensitivity in response to TRAIL, TNFα or anti-Fas activating antibody treatment, compared to 3D cultures of wild type cells (**Fig. 3D**).

Together, our results support a role for ERK5 kinase activity in conferring resistance to TRAIL-induced apoptosis in cancer cells, whereas ERK5 inhibition improves TRAIL anticancer activity by favoring caspase-8 activation.

ERK5 inhibition sensitizes EC patient-derived xenograft organoids (PDXOs) to TRAIL-induced toxicity.

To further explore the therapeutic potential of ERK5 inhibition as a rTRAIL sensitizer agent, we generated EC patient-derived xenograft organoids (PDXOs). The EC PDXOs mimic the architecture of the original tissue, reflect the genetic profile of endometrial tumors, and predict patient prognosis[38, 39]. Thus, PDXOs represent a highly relevant preclinical tool to study endometrial cancer. In this work we generated PDXOs from 2 different EC patients (**Suppl. Fig. 2**). Immunofluorescence analysis confirmed the structural organization of the cells into organoids, with the presence of two key glandular epithelial markers, EpCAM (**Fig. 4A**) and E-cadherin, as well as the mesenchymal and cytoskeleton markers vimentin and F-Actin, respectively (**Fig. 4B**). The positive and heterogeneous staining of the epithelial markers in our PDXOs recapitulated the morphological organization of endometrial tumors (**Fig. 4A-B**). Next, we tested the effect of ERK5i in PDXOs in combination with rTRAIL. To do so, we measured the viability of the PDXOs using two different techniques: quantification of the intracellular ATP (**Fig. 4C)**, and LIVE/DEAD cell viability assay (**Fig. 4D**). The PDXOs from the two patients showed different sensitivities to TRAIL, confirming that EC PDXOs exhibit patient-specific responses to drugs[38]. Thus, TRAIL treatment as a single agent decreased the viability of PDXOs from patient 440, but did not affect

bioRxiv preprint doi: https://doi.org/10.1101/2023.03.22.533738; this version posted March 24, 2023. The copyright holder for this preprint (which was not certified by peer review) is the author/funder, who has granted bioRxiv a license to display the preprint in perpetuity. It is made available under aCC-BY-NC-ND 4.0 International license.

viability of PDXOs from patient 1297 even at high concentrations (50 ng/ml). Interestingly, pre-incubation with the ERK5i sensitized both PDXOs to TRAIL-cytotoxicity (**Fig. 4B-C**). All in all, these preliminary results suggest that ERK5i could be a promising strategy to sensitize EC tumors to TRAIL anticancer activity, independently of the sensitivity status of the patients to TRAIL-treatment.

ERK5 inhibition or genetic deletion induces TP53INP2 protein levels to sensitize cancer cells to DR agonists.

TP53INP2 mediates caspase-8 K63-ubiquitylation in response to DR agonists, facilitating caspase-8 activation and apoptosis induced by these agonists[11]. Hence, to elucidate the mechanism involved in the sensitization to TRAIL exerted by ERK5 inhibition, we next investigated the effect of ERK5 modulation on TP53INP2 protein levels in four EC cell lines. Ishikawa, ARK1, ARK2 and AN3CA EC cells were treated with JWG-071 for 24h, and TP53INP2 protein levels were analyzed by immunoblot. ERK5i induced a robust increase on TP53INP2 protein levels in all EC cell lines tested (**Fig. 5A**), without affecting TRAIL receptor DR5 protein levels. Furthermore, genetic deletion of either ERK5 or MEK5 also resulted in a significant increase on TP53INP2 protein levels **(Fig. 5B**).

After DR receptor activation, DISC recruits and allows the activation of caspase-8, by a mechanism that is facilitated by the binding of TP53INP2 to caspase-8, which allows an efficient caspase-8 K63 ubiquitylation[11]. Therefore, we next tested whether increased TP53INP2 expression induced by the ERK5i also resulted in higher levels of TP53INP2 bound to caspase 8. For this purpose, cells transiently overexpressing FLAG-tagged TP53INP2 were treated with JWG-071 (6 h), and the amount of caspase 8 bound to TP53INP2 was detected by immunoblot of the immunoprecipitated pellets. As shown in **Fig. 5C**, ERK5 inhibition resulted in higher levels of TP53INP2/Caspase-8 complex.

Next, we investigated the role of TP53INP2 in the sensitization of EC cells to DR ligands exerted by ERK5 inhibition. We generated CRSIPR/Cas9 TP53INP2-KO Ishikawa cells, which were used to assess the apoptosis induced by DR agonists after pre-treatment with the ERK5i. Compared to wild type Ishikawa cells, TP53INP2-KO cells showed significantly lower apoptosis in response to TRAIL, TNFα or FasL **(Fig. 5D)**, confirming TP53INP2 as a player of the extrinsic apoptosis signaling pathway[11]. Importantly, the sensitization to DR agonists toxicity induced by ERK5 inhibition in EC cells was greatly impaired in cells where TP53INP2 was genetically depleted (TP53INP2-KO cells) **(Fig. 5D)**. These results were confirmed using cervical cancer HeLa cells with TP53INP2 knocked-down, where ERK5i resulted in impaired sensitization to DR agonists (**Fig. Suppl. 3)**. Accordingly, in TP53INP2-KO cells,

bioRxiv preprint doi: https://doi.org/10.1101/2023.03.22.533738; this version posted March 24, 2023. The copyright holder for this preprint (which was not certified by peer review) is the author/funder, who has granted bioRxiv a license to display the preprint in perpetuity. It is made available under aCC-BY-NC-ND 4.0 International license.

ERK5 inhibition did not enhance caspase-8 activity induced by DR agonists **(Fig. 5E-F)**. Finally, ERK5i sensitized Ishikawa-WT 3D cultures to TRAIL-induced toxicity, but not TP53INP2-KO 3D cultures **(Fig. 5G-H)**. These results indicate that TP53INP2 mediates the sensitization to DR agonists exerted by ERK5 inhibition, by favoring caspase-8 activation.

ERK5 phosphorylates and modulates TP53INP2 protein stability.

Given the fact that TP53INP2 has a short half-life (4 h[40]), and that ERK5 inhibition induced TP53INP2 protein levels, we next investigated whether ERK5 activity could regulate TP53INP2 protein stability. We first studied the role of the proteasome in TP53INP2 proteostasis using the inhibitor MG-132. To avoid an effect due to transcriptional regulation of the TP53INP2 gene, we used cells ectopically expressing human FLAG-TP53INP2. Short-time treatment (6 h) with the proteasome inhibitor MG-132 resulted in a robust increase on FLAG-TP53INP2 protein levels **(Fig. 6A)**. Of note, active ERK5 overexpression - but not ERK5 kinase-dead overexpression- resulted in impaired TP53INP2 protein levels, which were recovered by proteasome inhibition **(Fig. 6A).** We discarded a direct effect of MEK5 or ERK5 on the proteasome activity, since MEK5 or ERK5 inhibitors did not induce accumulation of cellular ubiquitylated proteins **(Fig. Suppl. 4).** These results strongly suggested that ERK5 kinase activity mediates the TP53INP2 ubiquitylation required for its proteasomal degradation. This was confirmed by denaturing pull-down assays using cells overexpressing His-tagged ubiquitin, TP53INP2 and/or active ERK5. As shown in **Fig. 6B**, proteasome inhibition increased TP53INP2 protein levels and induced accumulation of ubiquitylated species. Importantly, overexpression of active ERK5 resulted in significantly higher levels of ubiquitylated wild type TP53INP2 (**Fig. 6B),** suggesting that ERK5 activity induces TP53INP2 ubiquitylation and proteasomal degradation. Accordingly, active ERK5 did not induce degradation of the ubiquitylation-deficient TP53INP2-3K/R mutant[41] **(Fig. 6C),** whereas ERK5 inhibition restored the lower TP53INP2 protein levels induced by protein synthesis inhibition with cycloheximide (**Fig. 6D, upper panels)**. As expected, cycloheximide treatment did not affect protein expression of the ubiquitylation-deficient TP53INP2-3K/R mutant (**Fig. 6D, lower panels).**

Phosphorylation of KLF2 and cMYC by ERK5 regulates ubiquitylation and the proteostasis of these transcription factors[42, 43]. Given our results, we next explored whether this was also the case for TP53INP2. As it happens for other MAPKs, ERK5 requires to dock the substrate for an efficient phosphorylation. We performed immunoprecipitation assays using cell lysates containing endogenous **(Fig. 6E)** or overexpressed FLAG-tagged ERK5 and GST-tagged TP53INP2 proteins (**Fig. Suppl. 5**),

bioRxiv preprint doi: https://doi.org/10.1101/2023.03.22.533738; this version posted March 24, 2023. The copyright holder for this preprint (which was not certified by peer review) is the author/funder, who has granted bioRxiv a license to display the preprint in perpetuity. It is made available under aCC-BY-NC-ND 4.0 International license.

and we found that both proteins interact with each other. Next, we performed in vitro radiochemical kinase assays. We incubated affinity-purified TP53INP2 with pure recombinant active ERK5[44] in the presence of ^{32}P-[γATP]. After SDS-PAGE electrophoresis incorporation of ^{32}P into proteins was monitored by autoradiography. As shown in **Fig. 6F**, ERK5 efficiently phosphorylated TP53INP2 in vitro. TP53INP2 phosphorylation and ERK5 autophosphorylation were ablated with the ERK5 inhibitor JWG-071 (**Fig. 6F)**, indicating that trace contaminant kinases were not responsible for the phosphorylation.

To identify the TP53INP2 residues phosphorylated by ERK5, non-phosphorylated (control) and phosphorylated (ERK5) TP53INP2 were subjected to tryptic digestion and LC-MS/MS analysis. TP53INP2 is a proline-rich protein with low content of basic residues. Therefore, this analysis only allowed the identification of peptides comprising the N-term (aa 1-23) and C-term (aa 145-220) of TP53INP2, where Thr12, Ser14 and Ser208 were identified equally phosphorylated in both control and ERK5 samples **(Suppl. Fig. 6)**. These results suggested that ERK5 phosphorylates TP53INP2 in the central region of the protein comprising aa 24-144. As described for other MAPKs, ERK5 is a proline-directed kinase that phosphorylates Ser or Thr residues immediately preceded or followed by a proline residue[45]. TP53INP2 central region (aa 24-144) contains two clusters of Ser/Thr residues preceded or followed by a proline: cluster 1, containing Ser49, Ser65 and Thr74; and cluster 2, containing Ser94, Ser105, Ser121, Ser123 and Thr141. We first generated a TP53INP2 mutant in which the three putative phosphorylated sites in cluster 1 were mutated to Ala (TP53INP2-S49A/S65A/T74A, hereafter called TP53INP2-3A) (**Fig. 6G)**. The TP53INP2-3A mutant retained the ability to interact with ERK5 (**Suppl. Fig. 7)**, but it was poorly phosphorylated by ERK5 (**Fig. 6H)**, indicating that ERK5 at least phosphorylates Ser49, Ser65 and Thr74 in TP53INP2.

Next, we sought to investigate the impact of ERK5-mediated phosphorylation in TP53INP2 stability, by comparing the ectopic expression of wild type, phospho-deficient (3A) and ubiquitylation-deficient (3K/R) TP53INP2 mutants in cells. Interestingly, both the phospho-deficient and the ubiquitylation-deficient mutants showed similar expression, which was significantly higher than wild type TP53INP2 (**Fig**. **6I**). Furthermore, ERK5 inhibition increased the levels of wild-type TP53INP2 protein, but not of any of the mutants. Of note, ERK5 inhibition resulted in wild type TP53INP2 protein levels similar to those observed for basal expression of the 3A or 3K/R mutants **(Fig. 6I**). These results prompted us to investigate whether ERK5 phosphorylation affected TP53INP2 ubiquitylation. To address this question, we performed denaturing pull-down ubiquitin experiments. Both the ubiquitylation-deficient and the

bioRxiv preprint doi: https://doi.org/10.1101/2023.03.22.533738; this version posted March 24, 2023. The copyright holder for this preprint (which was not certified by peer review) is the author/funder, who has granted bioRxiv a license to display the preprint in perpetuity. It is made available under aCC-BY-NC-ND 4.0 International license.

phospho-deficient TP53INP2 mutants showed impaired ubiquitylation, compared to the wild type protein, suggesting that the phospho-deficient mutant showed impaired proteasomal degradation (**Fig. 6J**). To confirm this, we performed cycloheximide chase experiments. Ectopically expressed TP53INP2 showed a half-life of ~4 hours, while the phospho-deficient 3A mutant behaved as a significantly more stable protein (similar to the ubiquitylation-deficient mutant, half-life > 8 hours) **(Fig. 6K**). Together, our results suggest that phosphorylation at Ser49, 65 and Thr74 by ERK5 induces TP53INP2 ubiquitylation and proteasomal degradation.

ERK5 inhibition does not affect apoptosis-related transcriptional programs.

Next, to investigate changes on transcriptional programmes related to apoptosis due to ERK5 inhibition, we performed RNA sequencing (RNAseq) of EC Ishikawa cells treated with JWG-071. Only 260 genes were differentially expressed (DEG) in response to ERK5 inhibition (Qvalue<0.05, log_2 fold change >|1.5|) (**Fig. 7A)**, of which 202 (~80% of DEGs) were downregulated (**Figure 7B)**, suggesting that ERK5 kinase activity positively regulates transcription in EC cells. Of note, altered hallmarks include angiogenesis, p53-pathway and cholesterol hallmarks, but not the apoptosis hallmark (**Fig. 7C**). This was confirmed by Gene Set Enrichment Analysis (GSEA), which did not identify significant alterations (FDR=0.44) of apoptosis signatures in response to ERK5i (**Fig. 7D**). Further GSEA analysis did not find significant changes in extrinsic apoptosis transcriptional programs (**Fig. E-F**). Interestingly, ERK5i did not alter *TP53INP2* gene transcription, supporting a posttranslational regulation of TP53INP2 protein by ERK5.

Overall, our transcriptomic analysis supports the hypothesis that ERK5 modulates extrinsic apoptosis by posttranslational mechanisms, rather than altering transcription of apoptosis-related genes, at least in EC cells.

ERK5 inhibition or its genetic deletion sensitize EC cells to TRAIL/FasL expressed by natural killer cells.

Natural killer cells induce intrinsic and extrinsic apoptosis in cancer cells by two different mechanisms. Intrinsic apoptosis results from the action of the cytolytic pathway, which is induced by the release of granzymes and perforin. Perforin forms pores at the membrane of target cells, allowing the entry of granzymes that directly cleave and activate caspase-3. On the other hand, NK cells express membrane TRAIL and FasL, which bind DR4/5 (TRAIL receptors) and Fas (CD95) in target cells, triggering extrinsic apoptosis in tumor cells[46].

bioRxiv preprint doi: https://doi.org/10.1101/2023.03.22.533738; this version posted March 24, 2023. The copyright holder for this preprint (which was not certified by peer review) is the author/funder, who has granted bioRxiv a license to display the preprint in perpetuity. It is made available under aCC-BY-NC-ND 4.0 International license.

We next studied whether ERK5 inhibition sensitizes EC cells to apoptosis induced by NK cells. For this purpose, we expanded NK cells from freshly isolated PBMCs of four healthy human donors and purified them, as described in Methods; eNK cells displayed other phenotypic differences as compared to fresh NK cells (**Suppl. Fig 8)**, and expressed higher levels of activating receptors involved in the response to tumor cells (e.g. NKG2D, NKp46, NKp30)[47] (**Suppl. Fig 9 A-C)**. eNK cells expressed granzyme B and perforin (**Supp. Fig. 9 D and E)**. Unlike fresh NK cells, eNKs also displayed surface TRAIL (**Fig. 8A**) and FasL, the latter detected only following incubation with target cells (**Fig. 8B),** in agreement with a previous report[46].

Ishikawa EC cells were treated with the ERK5 inhibitor or vehicle, exposed to human eNKs, and apoptosis was quantified by measuring either caspase-8 activity with a luminescent substrate (LETD) or cleaved caspase-3 by flow cytometry intracellular staining (**Fig. 8C**). Gating strategy is exemplified in **Suppl. Fig. 10.** ERK5 inhibition increased eNK-induced caspase-8 activity in Ishikawa cells (**Fig. 8D**) and the relative effect was greater when perforin was inhibited with Concanamycin A[48] (**Fig. 8D,** yellow shading). Parallel experiments showed that ERK5i also tended to increase (but not significantly) eNKs-induced caspase-3 activity in Ishikawa cells, an effect which became particularly evident when the eNK cytolytic pathway was inhibited with Concanamycin A (**Fig. 8E)**. These results strongly suggest that ERK5 inhibition sensitizes EC cells to the extrinsic apoptosis induced by TRAIL and FasL expressed by NK cells. We also assessed the contribution of TP53INP2 to this process. Genetic deletion of TP53INP2 almost completely protected Ishikawa cells from apoptosis induced by eNK cell TRAIL/FasL **(Figure 8E)**. Of note, the ERK5 inhibitor did not sensitize TP53INP2-KO cells to apoptosis induced by TRAIL/FasL expressed by eNKs (**Figure 8E)**. These results support that ERK5 inhibition sensitizes EC cells to the toxicity induced by TRAIL/FasL from NK cells through TP53INP2. To further investigate the role of the MEK5-ERK5 pathway, analogous experiments were carried out using MEK5-KO or ERK5-KO EC cells. Similar to ERK5 inhibition, genetic deletion of MEK5 or ERK5 increased eNK cell-induced apoptosis of EC cells, particularly when the cytolytic pathway was inhibited **(Fig. 8F**).

Together, our results point to the ERK5-TP53INP2 pathway as a negative regulator of NK-TRAIL/FasL-induced apoptosis in cancer cells, and ERK5 inhibition as a new strategy to improve the anticancer activity of NKs.

Discussion

bioRxiv preprint doi: https://doi.org/10.1101/2023.03.22.533738; this version posted March 24, 2023. The copyright holder for this preprint (which was not certified by peer review) is the author/funder, who has granted bioRxiv a license to display the preprint in perpetuity. It is made available under aCC-BY-NC-ND 4.0 International license.

Extrinsic apoptosis is triggered by direct binding of DR ligands (TRAIL, TNFα and FasL) to their cognate receptors. After DR ligands interaction, DRs trimerize, inducing the formation of the DISC by recruiting FADD and the inactive form of caspase-8 (for TNFRs, recruitment of TRADD is necessary prior to FADD and pro-caspase-8 recruitment)[3]. Binding of multiple pro-caspase-8 molecules to FADD leads to caspase-8 oligomerization allowing its autoproteolytic cleavage[4]. Importantly, caspase-8 K-63 ubiquitylation plays a critical role in this process[9, 11]. Then, active caspase-8 cleaves the executioner caspase-3 to promote cellular apoptosis. In this study, we described a new signaling pathway involved in sensitization of cancer cells to the apoptosis induced by death receptor ligands. Hence, MAPK ERK5 phosphorylates and induces the ubiquitylation and proteasomal degradation of TP53INP2, a protein required for K63 ubiquitylation and full activation of caspase-8 in response to DR ligands (**Fig. 9**).

Recent work has described an important role for TP53INP2 in regulating the extrinsic apoptotic pathway. TP53INP2 binds to caspase-8, acting as a scaffolding protein that facilitates the recruitment of the E-3 ligase TRAF6[11]. TRAF6 mediates caspase-8 K63-linked ubiquitylation, required for caspase-8 oligomerization and full activation[36]. Thus, ectopic overexpression of TP53INP2 sensitized cancer cells to DR ligands-induced apoptosis[11], suggesting modulation of TP53INP2 proteostasis as a new strategy to improve the apoptosis induced by DR ligands. Here, we showed that cellular TP53INP2 has a short half-life (4 hours), is degraded at the proteasome upon ubiquitylation, and that phosphorylation regulates its stability. Specifically, we found that ERK5 phosphorylates at least three residues (S49, S65 and T74) located at the N-terminal end of TP53INP2, between the LC3-interacting region (LIR) and the ubiquitin interacting motif (UIM)[11]. Although we cannot discard the phosphorylation of other residues by ERK5, our results suggest that ERK5-mediated phosphorylation of S49, S65 and T74 is enough to induce TP53INP2 ubiquitylation and proteasomal degradation. Thus, it is likely that this multisite phosphorylation could allow the recruitment of the putative E3 ligase responsible for TP53INP2 ubiquitylation, yet to be discovered. In this regard, ERK5 is emerging as a protein kinase that regulates the stability of its substrates, as ERK5 phosphorylation modulates the recruitment of specific E3 ligases towards the target protein substrate. For instance, ERK5 phosphorylates KLF2 transcription factor at three Ser/Thr-Pro residues (T171, S175 and S247). This phosphorylation results in the recruitment of FBXW7 substrate adaptor of the RING-finger E3 ubiquitin ligase Cullin-1, which ubiquitylates and induces proteasomal degradation of KLF2[42]. On the contrary, phosphorylation of c-MYC at Ser62 by ERK5 impairs the recruitment of the FBXW7 substrate adaptor, which results in increased c-MYC protein

bioRxiv preprint doi: https://doi.org/10.1101/2023.03.22.533738; this version posted March 24, 2023. The copyright holder for this preprint (which was not certified by peer review) is the author/funder, who has granted bioRxiv a license to display the preprint in perpetuity. It is made available under aCC-BY-NC-ND 4.0 International license.

stability[43]. It will be interesting to investigate whether FBXW7 also regulates TP53INP2 ubiquitylation upon ERK5 phosphorylation.

In agreement with the results referred above, ERK5 pathway inhibition or genetic deletion sensitized cancer cells to DR ligands-induced apoptosis. This effect was mediated by the stabilization of TP53INP2 protein levels, since ERK5 pathway inhibition did not sensitize cancer cells lacking *TP53INP2* (TP53INP2-KO cells) to the apoptosis induced by DR ligands. Mechanistically, ERK5 pathway inhibition impaired TP53INP2 proteasomal degradation, which resulted in elevated TP53INP2 protein levels and higher TP53INP2-Caspase 8 complex levels. In this scenario, elevated TP53INP2 levels could facilitate the ubiquitylation and full activation of caspase-8 in response to DRs activation (**Fig. 9**). It will be interesting to investigate whether TP53INP2 stability is also regulated by other oncogenic protein kinases, as the MEK5-ERK5 pathway does. If so, TP53INP2 proteostasis could emerge as a central node regulating sensitivity/resistance to DR agonist cytotoxicity, by integrating oncogenic signaling pathways involved in cancer cell survival. Of note, we cannot rule out other players contributing to the sensitization to DR ligands-induced apoptosis exerted by inhibition of the ERK5 pathway. In this regard, transcriptomic analysis identified minor but significant changes on FLIP (log_2 FC -0,57) and XIAP (log_2 FC -0,27) mRNA levels in response to ERK5 inhibition, two key proteins involved on resistance to DR ligands cytotoxicity[49]. Future work is needed to investigate whether ERK5 inhibition impairs FLIP and XIAP protein level, as observed for the CDK1/2/9 and ERK5 multiple kinase inhibitor TG02[50].

Among DR ligands, only TRAIL-receptor agonists (TRAs) have been developed as anticancer agents. Although FasL and TNFα show potent cytotoxicity in cancer cells, the use of these DR agonists in the clinic has been jeopardized by their severe toxicity in normal cells and tissues. Among others, TNF-α and FasL are cytotoxic towards hepatocytes, and induce lethal liver injuries in animal models[51, 52]. On the contrary, TRAIL selectively induces apoptosis in cancer cells[12], and therefore TRAs represent a promising strategy to tackle cancer. However, despite initial hopes, TRAs have shown limited therapeutic benefits in clinical trials due to inherent resistance of primary tumors to TRAIL-treatment[53]. Consequently, much effort has been addressed to identify strategies to improve the anticancer activity of TRAs, mostly by sensitizing cancer cells to TRAs-induced apoptosis. Initially, strategies addressed specific resistance mechanisms driven by anti-apoptotic proteins such as IAPs and Bcl-2 family members. However, due to the heterogeneous nature of human cancers, these strategies did not show benefit in clinical trials[54]. Lately, it has been proposed the use of protein kinase inhibitors to remove

bioRxiv preprint doi: https://doi.org/10.1101/2023.03.22.533738; this version posted March 24, 2023. The copyright holder for this preprint (which was not certified by peer review) is the author/funder, who has granted bioRxiv a license to display the preprint in perpetuity. It is made available under aCC-BY-NC-ND 4.0 International license.

resistance to TRAs-based therapies, given their ability to simultaneously block both oncogenic pathways and the activity of several proteins involved in this resistance[13]. In this work, using cancer cell lines from different origin and known to be resistant to recombinant TRAIL (rTRAIL), we demonstrated that pharmacologic inhibition of ERK5 is an effective strategy to improve TRAIL cytotoxicity, by stabilizing TP53IP2 protein levels. Interestingly, ERK5 inhibition or MEK5 genetic deletion also sensitized NSCLC KRAS mutated A549 cells to TRAIL cytotoxicity, a model where TRAIL induces cancer progression, invasion and metastasis instead of activating apoptosis[53, 55]. These preliminary results suggest that ERK5 inhibition switches the protumoral phenotype of TRAIL to an antitumoral (apoptotic) phenotype in NSCLC harboring activating KRAS mutations. We also found that ERK5 inhibition sensitized EC patient-derived xenografts (PDXOs, a highly relevant pre-clinical model) to rTRAIL toxicity. Since EC PDXs maintain the genomic and molecular characteristics of patients[39], and PDXOs maintain the genetic profile of EC subtypes predicting patient prognosis against treatments[38], our results support the use of ERK5 inhibitors to sensitize EC tumors to TRAs-based therapies. Future work is required to investigate whether this strategy might work for other cancer types.

Natural killer cells are critical players of the anti-tumor action of the immune system. Lately, NK cells have gained significant attention for cancer immunotherapy, since their cytotoxic activity does not require prior exposure to tumor antigens and they can efficiently kill tumor cells with minimal graft-versus-host disease[56]. However, one limitation of NK cell-based immunotherapy is that tumor cells frequently escape the immune attack due to inherent resistance mechanisms to apoptosis[57]. Therefore, drugs that sensitize tumors to the NK cytotoxicity are gaining high clinical relevance. Here, we provide preliminary evidence showing that ERK5 inhibition sensitizes EC cells to the extrinsic apoptosis (caspase-8 activation) induced by TRAIL/FasL expressed by eNKs. Our results are in agreement with a previous report, showing that ERK5 silencing (shRNA) sensitized leukemic cells to the cytotoxicity exerted by the cytolytic and the extrinsic apoptotic (FasL) pathways of NK cells[58], although the authors did not deep into the mechanistics of such effect. Our study points TP53INP2 protein as the key player in this process. As it happened for rTRAIL and anti-Fas activating antibody, sensitization of EC cells to NK cells required TP53INP2 protein stabilization. Our results suggest that the enhanced eNK-induced apoptosis observed upon ERK5 blockade is due to an effect on the TRAIL/FasL-induced extrinsic pathway rather than on intrinsic apoptosis induced by perforin and granzymes, an important cytotoxic mechanism of NK cells. However, ERK5 inhibitors might well be relevant for improving the efficacy of

bioRxiv preprint doi: https://doi.org/10.1101/2023.03.22.533738; this version posted March 24, 2023. The copyright holder for this preprint (which was not certified by peer review) is the author/funder, who has granted bioRxiv a license to display the preprint in perpetuity. It is made available under aCC-BY-NC-ND 4.0 International license.

NK-based immunotherapies, given the fact that NK cells switch from granzyme/perforin-mediated cancer cell death to TRAIL/FasL-induced cytotoxicity during subsequent tumor cell encounters (also called serial killing)[46]. In this regard, it will be important to investigate whether modulation of the ERK5-TP53INP2 pathway also affects the expression of components of both cytolytic (Granzymes/perforin) and TRAIL/FasL pathways in NK cells. Whether the results observed with our preparations of eNK cells might be extrapolated to different clinical adoptive immunotherapy protocols deserve attention[59].

The MEK5-ERK5 pathway plays an important role regulating the proliferation and survival of many solid cancers, such as hepatocarcinoma[18], prostate[21] or endometrial cancer[20], among others. Consequently, ERK5 has been proposed as a new target to tackle several solid cancers. Thus, MEK5 or ERK5 pharmacologic inhibitors have shown anticancer activity in xenograft models of several cancers. Of relevance for our work, ERK5 inhibitors sensitize tumor xenografts to standard chemotherapics such as 5-fluorouracil[60], doxorubicin[61], paclitaxel[20] or docetaxel[62], potentiating the intrinsic apoptosis exerted by chemotherapy treatments. In this work, we provide for the first time evidence supporting a role for ERK5 in sensitizing cancer cells to activators of the extrinsic apoptotic pathway. Hence, we propose pharmacologic modulation of ERK5 kinase activity as an effective way to improve the anticancer efficacy of apoptosis activating drugs, and support further preclinical development of ERK5 inhibitors.

bioRxiv preprint doi: https://doi.org/10.1101/2023.03.22.533738; this version posted March 24, 2023. The copyright holder for this preprint (which was not certified by peer review) is the author/funder, who has granted bioRxiv a license to display the preprint in perpetuity. It is made available under aCC-BY-NC-ND 4.0 International license.

Methods

Reagents. ERK5 inhibitors JWG-071 (Merck), AX-15836 (MedChemExpress), and MEK5 inhibitors BIX02188 and BIX02189 (Selleckchem) were diluted in dimethyl sulfoxide (DMSO, Sigma). Pan-caspase inhibitor Q-VD(OMe)-OPh (APExBIO) was diluted in DMSO. Death-receptor agonists, TRAIL (Peprotech) and TNFα (Merck) were diluted in H_2O 0.1% BSA, and anti-Fas activating antibody (Merck) was diluted in 50% glycerol in PBS.

DNA constructs. The pEBG2T vectors encoding GST-tagged human ERK5 (WT) and ERK5 kinase-dead mutant (D200A) were a gift from Dr. P. Cohen (MRC Protein Phosphorylation Unit, Dundee, UK)[44]. The pCMV5 vector encoding for HA-tagged constitutively active MEK5 (MEK5DD) was a gift from Dr. E. Nishida (Kyoto University, Japan)[63]. The vectors encoding human N-Terminal FLAG-tagged TP53INP2 were generated by inserting the human TP53INP2 full-length coding sequence into a pCDNA3.1 vector, using the restriction sites NheI and XhoI. The FLAG-tagged human TP53INP2 mutants 3A (Ser49Ala, Ser65Ala, Thr74Ala) and 3K/R (Lys 165/187/204 mutated to Arg) were generated using the same strategy, inserting the synthetic sequences (ProteoGenix) into a pCDNA3.1 vector. The pCMV vector encoding 6xHis-tagged ubiquitin was a gift from Dr. A. C. Vertegaal (Leiden University, Netherlands)[64],

Cells, cell culture and transfection. AN3CA, ARK1 and ARK2 endometrial cancer (EC) cells, HeLa cervical cancer cells, A549 non-small cell lung cancer cells, LnCaP prostate cancer cells and SK-N-AS neuroblastoma cells were purchased from ATCC. Ishikawa EC cells were from ECACC and were purchased from Sigma. HeLa, ARK1, ARK2 and A549 cells were maintained in Dulbecco's Modified Eagle's Medium (DMEM; Thermofisher) supplemented with 10% foetal bovine serum (FBS; Gibco) and 1% Penicillin/Streptomycin (Pen/Strep; Gibco). AN3CA were maintained in DMEM-F12 medium (ThermoFisher) supplemented with 10% FBS and 1% Pen/Strep. SK-N-AS cells were cultured in Iscove′s Modified Dulbecco′s medium (IMDM; Thermofisher) with 20% FBS (Gibco), 1% Pen/Strep (Gibco) and 1% Insulin-Transferrin-Selenium (Gibco). Ishikawa cells were maintained in Modified Eagle Medium (MEM; Thermofisher). LnCaP cells were maintained in Roswell Park Memorial Institute Medium (RPMI-1640; Gibco) supplemented with 10% FBS (Sigma), 1% Pen/Strep (Gibco), nonessential amino acids (NEAA; Sigma), sodium pyruvate (Gibco) and HEPES (Gibco). HEK293T cells were transfected using Polyethylenimine (PEI; Polysciences), and Ishikawa and AN3CA cells were transfected using Lipofectamine2000™ (Thermofisher) as described before[65].

bioRxiv preprint doi: https://doi.org/10.1101/2023.03.22.533738; this version posted March 24, 2023. The copyright holder for this preprint (which was not certified by peer review) is the author/funder, who has granted bioRxiv a license to display the preprint in perpetuity. It is made available under aCC-BY-NC-ND 4.0 International license.

For 3D cultures of EC cells, a Matrigel (Corning) layer of approximately 1-2 mm in thickness was seeded per well in a 96-well plate. After solidification of the Matrigel layer at 37ºC, 2500 Ishikawa cells were seeded per well in basal medium (DMEM/F-12, 1mM sodium pyruvate, 1% Pen/Strep) supplemented with 2% dextran-coated charcoal-stripped serum (Cytiva) and 3% Matrigel. 3D cultures were then left to grow during 5-7 days before performing the corresponding viability experiments.

Generation of MEK5, ERK5 and TP53INP2 knockout cells by CRISPR/Cas9 technology. We used CRISPR/Cas9 technology to genetically delete the MEK5 gene (*MAP2K5*) in HeLa, Ishikawa and A549 cells, the ERK5 gene (MAPK7) in Ishikawa cells, and the TP53INP2 gene (*TP53INP2*) in Ishikawa cells. We used the following commercial kits from Santa Cruz technology: MEK5 (sc-401688-KO and sc-401688-HDR), ERK5 (sc-400891-KO and sc-400891-HDR) and TP53INP2 (sc-405261-KO-2 and sc-405261-HDR-2). Briefly, cells were co-transfected with the KO plasmid (containing the sgRNAs for the specific gene and the Cas9 endonuclease gene) and the HDR plasmid (which contains puromycin-resistance gene that is inserted into the cut sites of the target genes through a HDR mechanism). The KO cells acquiring the puromycin resistance gene were selected with 1 ug/ml of puromycin (Sigma) for ~3 weeks. Single colonies were recovered, monitored for target gene expression, and further expanded and stored in liquid nitrogen.

Cell lysis, immunoblotting and immunoprecipitation. For immunoblot analysis cells were lysed in ice-cold RIPA buffer supplemented with 50 mM NaF, 5 mM sodium-pyrophosphate and 1 mM sodium-orthovanadate. Cell lysates were sonicated and centrifuged at 12.000 g for 12 min at 4ºC, and supernatants were stored at -20°C until use. Protein concentration was determined using Pierce™ Coomassie Plus reagent (Thermofisher). Proteins were resolved in SDS-PAGE gels and electrotransferred onto nitrocellulose membranes (Merck). After incubation with the appropriated primary antibody, detection was performed using horseradish peroxidase-conjugated secondary antibodies and enhanced chemiluminescence reagent (Bio-Rad). Primary and secondary antibodies used are given in **Suppl. Table 1.**

For immunoprecipitation, cells were lysed in ice-cold NP-40 buffer (50 mM Tris-HCl, 0.27M Sucrose, 1mM orthovanadate, 1mM EDTA, 1mM EGTA, 10 mM glycerol-phosphate disodium salt, 50 mM NaF, 5 mM sodium pyrophosphate, 0.5% (w/v) NP40, pH 7.5). Protein G-sepharose beads (Cytiva) bound to 2.5 ug of the corresponding antibody were incubated with 1 mg of cell lysate for 2h at 4ºC with rotation. Then, immunoprecipitates were washed twice with NP-40 buffer supplemented with 150 mM NaCl, and

bioRxiv preprint doi: https://doi.org/10.1101/2023.03.22.533738; this version posted March 24, 2023. The copyright holder for this preprint (which was not certified by peer review) is the author/funder, who has granted bioRxiv a license to display the preprint in perpetuity. It is made available under aCC-BY-NC-ND 4.0 International license.

once with kinase buffer (Tris-HCl 50 mM, 0.1 mM EGTA, pH 7.5). Proteins were then eluted with Laemmli buffer and boiled for 5 min at 95ºC. Immunoprecipitation of cell lysates overexpressing FLAG-tagged or GST-tagged proteins were performed using anti-FLAG-M2 affinity beads (Merck) or glutathione-Sepharose beads (Cytiva).

Cell viability and clonogenic assays. Cell viability was determined using the MTT (3-(4,5-dimethyl-2-thiazolyl)-2,5-diphenyl-2H-tetrazolium Blue, Sigma) reduction assay. For clonogenic assays, 1000 Ishikawa cells were seeded in 6-wells plates. Twenty-four hours later, cells were treated with the indicated treatments for 10 days and stained with 0.5% crystal violet solution. Colonies were counted using ImageJ (FiJi).

Flow cytometry analysis of apoptosis. Apoptosis analysis was performed using an Annexin-V Apoptosis detection kit (Invitrogen). Briefly, treated cells were trypsinized and counted. 10^5 cells were selected for the staining. Cells were washed with PBS, twice with the binding buffer, and finally incubated with Annexin-V-APC and PI for 15 minutes. Samples were then acquired on a BD LSRFortessa (BD Biosciencies) flow cytometer and analyzed with FlowJo software (vX.0.7, TreeStar).

Caspase-8 activity assay. Cells were cultured in 96-well white plates with clear bottom (Corning). Twenty-four hours later, cells were treated, and caspase-8 activity was measured using the Caspase-Glo® 8 kit (Promega), which uses the specific caspase-8 substrate LETD sequence, following the manufacturer's instructions. Luminescence was measured in a Spark microplate reader (TECAN).

In vitro radiochemical ERK5 kinase activity assay. Lysates from HEK293 cells overexpressing FLAG-tagged wild typeTP53INP2 or the TP53INP2-3A were affinity-purified with anti-FLAG-M2 affinity beads (Merck). Then, beads containing the immunoprecipitated TP53INP2 proteins were incubated with 200 ng of active ERK5[44] in kinase buffer. Reactions (total volume 50 μL) were started by adding a mixture of 10 mM $MgCl_2$, 200 μM [γ-^{32}P]-ATP (400 cpm/pmol). Assays were carried out at 30ºC for 15-30 min and terminated by adding 5x Laemmli buffer. Finally, samples were boiled for 5 min at 95ºC, resolved by SDS/PAGE gel electrophoresis, and radioactivity detected by autoradiography.

In vivo TP53INP2 ubiquitination assay. HEK293T cells overexpressing His-Tagged Ubiquitin, FLAG-TP53INP2 and/or GST-ERK5 and HA-MEK5DD (constitutively active), were resuspended in 1 ml of Buffer A (6M guanidinium-HCl, 100 mM Na2HPO4/NaH2PO4, 10 mM Imidazole, pH 8), sonicated for 1 minute, passed through a 25G syringe, and finally centrifuged for 15 min at 15.000 g. The resulting

bioRxiv preprint doi: https://doi.org/10.1101/2023.03.22.533738; this version posted March 24, 2023. The copyright holder for this preprint (which was not certified by peer review) is the author/funder, who has granted bioRxiv a license to display the preprint in perpetuity. It is made available under aCC-BY-NC-ND 4.0 International license.

supernatants were incubated with 25 ul of Ni^{2+}-NTA-agarose beads for 2 h at room temperature with rotation. Beads were successfully washed as follows: twice with Buffer A, four times with Buffer B (buffer A diluted 1:3 in buffer C (25 mM Tris-HCl, 20 mM Imidazole, pH 6.8), and twice with buffer C. Ubiquitylated proteins were eluted with Buffer C containing 250 mM Imidazole for 15 min at 37ºC. After adding Laemmli buffer, eluted proteins were boiled for 5 min at 95ºC, resolved in a SDS/PAGE gel and immunoblotted using anti-TP53INP2 antibody.

Phosphoproteomic analysis. Purified FLAG-tagged TP53INP2 was incubated with 200 ng of active ERK5 in kinase buffer with 200 µM ATP for 30 min at 30°C, in a total reaction volume of 50 µl. The reaction was terminated by adding 5x Laemmli buffer, samples resolved in SDS/PAGE gel electrophoresis and stained with Coomassie Blue. The band corresponding to TP53INP2 was excised and digested with sequencing grade modified trypsin (Promega), using LFASP digestion protocol. Extracted peptides were analyzed by label-free liquid chromatography-tandem mass spectrometry (LC-MS/MS) at the LP-CSIC/UAB Service facility. LC-MS/MS was performed using an Agilent 1200 nanoflow system (Agilent Technologies) coupled to an LTQ-Orbitrap XL mass spectrometer (Thermo Fisher Scientific) equipped with a nanoelectrospray ion source (Proxeon Biosystems). Peptides were identified using Proteome Discoverer v1.4 and SwissProt human database, and analyzed using MASCOT database search (matrixscience.com) to identify phospho-Ser/Thr and phospho-Tyr.

Generation of EC Patient-Derived Xenograft Organoids (PDXOs). Each tumor tissue from EC PDXs was transferred into a 50-ml Falcon tube containing washing medium (DMEM/F12 supplemented with 1% L-glutamine, Penicillin-Streptomycin and 10 mM HEPES) and kept on ice until the start of the isolation. Tissues were minced using scalpels, followed by sedimentation with washing medium supplemented with 0.1% BSA during 2-3 min, to wash away any potential microorganisms or cell types not contributing to the establishment of organoids. Enzymatic digestion was done with 1.25 U/ml dispase II (Merck), 0.4 mg/ml collagenase from Clostridium histolyticum type V (Merck), and ROCK inhibitor Y-27632, on an orbital shaker for 60 min at 37 °C. Undigested tissue was discarded using a 100 µm cell strainer, and red blood cell lysis buffer (Merck) was subsequently added to the pellet. Single cells were then resuspended in BME (basement membrane extract, Bio-Techne) and seeded (20 µl droplets) onto non-treated 12-well culture plates. The suspension of organoids and BME was solidified at 37 °C for 10-15 min before covering each well with 750 µl of standard organoid medium containing washing medium supplemented with 100 ng/ml recombinant human EGF (Bio-Techne), recombinant human Noggin (100

bioRxiv preprint doi: https://doi.org/10.1101/2023.03.22.533738; this version posted March 24, 2023. The copyright holder for this preprint (which was not certified by peer review) is the author/funder, who has granted bioRxiv a license to display the preprint in perpetuity. It is made available under aCC-BY-NC-ND 4.0 International license.

ng/ml, Stemcell Technologies), B-27 supplement (ThermoFisher), 10 μM Y-27632 (Miltenyi Biotec), 100 nM SB202190 (Merck), 10 nM 17-β Estradiol (Merck), 10 μM Nicotinamide (Merck), 500 nM A83-01 (Merck) and N-acetyl-L-cysteine 1.25mM (Merck).

Viability assays in 3D cultures and EC PDXOs. Cells were seeded in 96-well white plates with clear bottom (Corning). When the 3D cultures or organoids were formed, they were treated for the indicated times and viability was assessed using the CellTiter-Glo® 3D Cell viability kit (Promega), following the manufacturer's instructions. The CellTiter-Glo® 3D Cell viability kit measures the intracellular ATP content of the 3D cultures which is directly related to the viability of the cells. Luminescence was measured in a Spark microplate reader (TECAN). In parallel experiments, viability measurement was performed using a LIVE/DEAD viability/cytotoxicity kit assay (Thermofisher), as described before[65].

EC PDXOs immunofluorescence microscopy. Organoids were extracted from their BME matrix by adding ice-cold cell recovery solution (Corning) for 30-60 minutes. This procedure enables the dissolution of BME without damaging the organoids, and allows an optimal penetration of the antibody. Then, organoids were fixed with 4% (w/v) paraformaldehyde at 4°C for 45 min. Throughout the protocol, samples were washed extensively to avoid background or loss of signal. Primary antibodies E-cadherin (Abcam), Vimentin (Abcam) and EpCAM (Cell Signalling) were incubated overnight at 4°C on a horizontal shaker (40 rpm). Secondary antibodies Mouse IgG Alexa Fluor 555 (Abcam), Rabbit IgG Alexa Fluor 488 (Abcam) and the Phalloidin-iFluor 647 (Abcam) were added to each well and incubated overnight in the same conditions. Antibodies used in this process are listed in **Suppl. Table 2**. Optical clearing was accomplished by resuspending the organoids with homemade fructose-glycerol clearing solution. For slide preparation, a slice of double-sided tape was added on both sides of the slide to lift the coverslip, thereby maintaining the 3D structure of the organoids. The slide was then visualized by fluorescence confocal microscopy (Zeiss LSM980).

RNA-seq analysis. Ishikawa cells were treated with either vehicle or JWG-071 for 24 h, and then lysed for RNA purification. RNA was purified from Ishikawa cells using RNeasy kit (Qiagen). RNA quality was evaluated using a Bioanalyzer 2100 (Agilent), and samples with a RIN value higher than 7 were selected. Then, libraries were prepared using TruSeq Kit (Illumina). RNA-sequencing (30 million reads per sample) was carried out at the DNBseq™ NGS technology platform with the Ilumina HiSeq4000 at the Beijing Genomics Institute (BGI). Finally, functional enrichment analyses were performed using Dr.

bioRxiv preprint doi: https://doi.org/10.1101/2023.03.22.533738; this version posted March 24, 2023. The copyright holder for this preprint (which was not certified by peer review) is the author/funder, who has granted bioRxiv a license to display the preprint in perpetuity. It is made available under aCC-BY-NC-ND 4.0 International license.

Tom software (BGI), the gene set enrichment analysis (GSEA) software and the gene ontology (GO) collection (MSigDB v7.1).

Natural killer cell amplification and immunophenotyping characterization. Freshly isolated PBMCs (peripheral blood mononuclear cells) from healthy human donors were co-cultured with irradiated (40 Gy) RPMI 8866 B lymphoblastoid cell line in a ratio 3:1 ($3x10^6$ PBMCs and $1x10^6$ 8866 cells per well in a 12 well-plate) in RPMI 1640 GlutaMax (Thermo Fisher Scientific) supplemented with penicillin (100 U/ml), streptomycin (100 µg/ml), sodium pyruvate (1 mM), and 10% FBS. Cultures were split and fed every 3-4 days, adding IL-2 (200 U/ml) from day 7. On day 12, cultures were harvested and expanded natural killer (eNK) cells ($CD56^+/CD3^-$) were purified (Human NK Cell Isolation kit, Miltenyi). Expression of cytotoxic markers (Granzyme B, Perforin, TRAIL and FasL), activating (NKG2D, NKp46, NKp30, CD16) and inhibitory (KIRs, ILT2, NKG2A) NK cell receptors (NKR), as well as the CD57 marker was assessed. Briefly, PBMC or eNK cells were treated with blocking buffer (2% FBS, 2mM EDTA, 10 µg/mL aggregated human IgG in PBS) and stained with the indicated labelled antibodies listed in Supplementary table 2. For intracellular staining, cells were fixed and permeabilized with Fix/Perm kit (BD Biosciences) and stained for intracellular antigens. Samples were acquired on a BD-LSRII (BD Biosciences) and analyzed with FlowJo software (vX.0.7, TreeStar). Antibodies used in this process are listed in **Suppl. Table 3**.

Natural killer cell cytotoxicity assay. Ishikawa cells were pre-treated with either JWG-071 or vehicle (0.05% v/v DMSO) for 12h and detached. In parallel, eNK cells were pre-treated with 1 µM Concanamycin-A (MedChemExpress) or vehicle (0.1% v/v DMSO) for 2 hours. eNK cells were co-cultured with Ishikawa EC cells at 1:5 (effector:target) ratio in the presence of 1 µM Concanamycin A or vehicle for 4 hours in U-bottom 96-well plates (Corning), and active-caspase-3 in Ishikawa cells was analyzed by flow cytometry. Briefly, samples were stained with mAbs specific for CD45-BV510 (clone HI30) and EpCAM-AF647 (clone 9C4), together with Near IR-fluorescent reactive dye (Invitrogen) to exclude dead cells, permeabilized with wash/perm buffer, stained with anti-cleaved caspase-3-FITC antibody (BD Pharmingen, clone C92-605), acquired on a BD-LSRII flow cytometer (BD Biosciences) and analyzed with FlowJo software (vX.0.7, TreeStar). Percentages of active Caspase 3+ cells were assessed in viable Ishikawa cells ($EpCAM^+/CD45^-$). Antibodies used in this process are listed in **Suppl. Table 3**.

bioRxiv preprint doi: https://doi.org/10.1101/2023.03.22.533738; this version posted March 24, 2023. The copyright holder for this preprint (which was not certified by peer review) is the author/funder, who has granted bioRxiv a license to display the preprint in perpetuity. It is made available under aCC-BY-NC-ND 4.0 International license.

Schematics and statistical analysis. The schemes in figures 6F, 8C and 9 were created with PowerPoint (Microsoft). Individual data points are displayed in all the bar plots. Data are presented as the mean ± standard deviation (S.D.) of at least n=3 independent experiments. The statistical tests used are reported in the figure legends. Significance was established using one-way ANOVA followed by Bonferroni multiple comparison test, two-tailed Student's test or two-way ANOVA followed by Tukey multiple comparison test (individual p-values are represented in each figure). All the analyses were performed with GraphPad Prism 8.

Data availability. The RNA sequencing datasets generated in this study have been deposited in the GEO database repository under accession code (pending). The remaining data are available within the Article, Supplementary Information or Dataset files.

bioRxiv preprint doi: https://doi.org/10.1101/2023.03.22.533738; this version posted March 24, 2023. The copyright holder for this preprint (which was not certified by peer review) is the author/funder, who has granted bioRxiv a license to display the preprint in perpetuity. It is made available under aCC-BY-NC-ND 4.0 International license.

Acknowledgments

S.E.G. and A.G.G: are recipients of a fellowship from FI-AGAUR (2020-FISDU-00575 and FI_B 00293, respectively). I.B.A. is recipient of a PIF fellowship from UAB. M.V.C is recipient of a PFU fellowship (Ref. FPU21/01999). B.V.M. is recipient of a PFIS fellowship (ref. FI21/00271). We thank Miguel Segura and Guillermo Yoldi for helpful discussions. We also thank the VHIR High Technology Unit (UAT) core facilities and staff, and the LP-CSIC/UAB Proteomic Laboratory for proteomics analyses.

Funding

J.M.L. acknowledges support from Spanish Ministry of Economy and Competitiveness (MINECO, SAF2015-64237-R), Spanish Ministry of Science and Innovation (PID2019-107561RB-I00), and co-funded by the European Regional Development Fund (ERDF, "A way to make Europe"/"Investing in your future"). E.C. was founded by Fundación Científica Asociación Española Contra el Cáncer (AECC, GCTRA1804MATI) and Generalitat de Catalunya (2021-SGR-01157). A.Z. acknowledges support by research grants from MINECO (PID2019-106209RB-I00), CIBERDEM ("Instituto de Salud Carlos III"), and from an ICREA "Academia" Award (Generalitat de Catalunya). M.L.B. acknowledges support by research grant PID2019-110609RB-C21 from MCIN/AEI/ 10.13039/501100011033.

Author contributions

Conceptualization: S.E.G., J.M.L. Investigation: S.E.G., S.I., E.A.P., M.D., B.V.M., M.V.C., I.B.A., A.G.G. Resources: J.M.L., A.Z., M.L.B., E.C. Funding acquisition: J.M.L., A.Z., M.L.B., E.C. Formal analysis: S.E.G., J.M.L. Writing: S.E.G., J.M.L. Supervision: J.M.L. All the authors read, critically revised, and approved the final manuscript.

Competing interest

Authors declare no competing interest.

References

bioRxiv preprint doi: https://doi.org/10.1101/2023.03.22.533738; this version posted March 24, 2023. The copyright holder for this preprint (which was not certified by peer review) is the author/funder, who has granted bioRxiv a license to display the preprint in perpetuity. It is made available under aCC-BY-NC-ND 4.0 International license.

1. Li, P. *et al.* Cytochrome c and dATP-dependent formation of Apaf-1/caspase-9 complex initiates an apoptotic protease cascade. *Cell* **91**, 479-489 (1997).

2. Zou, H., Li, Y., Liu, X. & Wang, X. An APAF-1.cytochrome c multimeric complex is a functional apoptosome that activates procaspase-9. *J Biol Chem* **274**, 11549-11556 (1999).

3. Medema, J.P., Scaffidi, C., Krammer, P.H. & Peter, M.E. Bcl-xL acts downstream of caspase-8 activation by the CD95 death-inducing signaling complex. *J Biol Chem* **273**, 3388-3393 (1998).

4. Dickens, L.S. *et al.* A death effector domain chain DISC model reveals a crucial role for caspase-8 chain assembly in mediating apoptotic cell death. *Mol Cell* **47**, 291-305 (2012).

5. Fox, J.L. *et al.* Cryo-EM structural analysis of FADD:Caspase-8 complexes defines the catalytic dimer architecture for co-ordinated control of cell fate. *Nat Commun* **12**, 819 (2021).

6. Li, H., Zhu, H., Xu, C.J. & Yuan, J. Cleavage of BID by caspase 8 mediates the mitochondrial damage in the Fas pathway of apoptosis. *Cell* **94**, 491-501 (1998).

7. Schug, Z.T., Gonzalvez, F., Houtkooper, R.H., Vaz, F.M. & Gottlieb, E. BID is cleaved by caspase-8 within a native complex on the mitochondrial membrane. *Cell Death Differ* **18**, 538-548 (2011).

8. Gonzalvez, F. *et al.* TRAF2 Sets a threshold for extrinsic apoptosis by tagging caspase-8 with a ubiquitin shutoff timer. *Mol Cell* **48**, 888-899 (2012).

9. Jin, Z. *et al.* Cullin3-based polyubiquitination and p62-dependent aggregation of caspase-8 mediate extrinsic apoptosis signaling. *Cell* **137**, 721-735 (2009).

10. He, L., Wu, X., Siegel, R. & Lipsky, P.E. TRAF6 regulates cell fate decisions by inducing caspase 8-dependent apoptosis and the activation of NF-kappaB. *J Biol Chem* **281**, 11235-11249 (2006).

11. Ivanova, S. *et al.* Regulation of death receptor signaling by the autophagy protein TP53INP2. *EMBO J* **38** (2019).

12. Ashkenazi, A. & Dixit, V.M. Apoptosis control by death and decoy receptors. *Curr Opin Cell Biol* **11**, 255-260 (1999).

13. Montinaro, A. & Walczak, H. Harnessing TRAIL-induced cell death for cancer therapy: a long walk with thrilling discoveries. *Cell Death Differ* (2022).

bioRxiv preprint doi: https://doi.org/10.1101/2023.03.22.533738; this version posted March 24, 2023. The copyright holder for this preprint (which was not certified by peer review) is the author/funder, who has granted bioRxiv a license to display the preprint in perpetuity. It is made available under aCC-BY-NC-ND 4.0 International license.

14. Drew, B.A., Burow, M.E. & Beckman, B.S. MEK5/ERK5 pathway: the first fifteen years. *Biochim Biophys Acta* **1825**, 37-48 (2012).

15. Kato, Y. *et al.* BMK1/ERK5 regulates serum-induced early gene expression through transcription factor MEF2C. *EMBO J* **16**, 7054-7066 (1997).

16. Gomez, N., Erazo, T. & Lizcano, J.M. ERK5 and Cell Proliferation: Nuclear Localization Is What Matters. *Front Cell Dev Biol* **4**, 105 (2016).

17. Stecca, B. & Rovida, E. Impact of ERK5 on the Hallmarks of Cancer. *Int J Mol Sci* **20** (2019).

18. Rovida, E. *et al.* The mitogen-activated protein kinase ERK5 regulates the development and growth of hepatocellular carcinoma. *Gut* **64**, 1454-1465 (2015).

19. Montero, J.C. *et al.* Expression of Erk5 in early stage breast cancer and association with disease free survival identifies this kinase as a potential therapeutic target. *PLoS One* **4**, e5565 (2009).

20. Dieguez-Martinez, N. *et al.* The ERK5/NF-kappaB signaling pathway targets endometrial cancer proliferation and survival. *Cell Mol Life Sci* **79**, 524 (2022).

21. McCracken, S.R. *et al.* Aberrant expression of extracellular signal-regulated kinase 5 in human prostate cancer. *Oncogene* **27**, 2978-2988 (2008).

22. Pi, X., Yan, C. & Berk, B.C. Big mitogen-activated protein kinase (BMK1)/ERK5 protects endothelial cells from apoptosis. *Circ Res* **94**, 362-369 (2004).

23. Girio, A., Montero, J.C., Pandiella, A. & Chatterjee, S. Erk5 is activated and acts as a survival factor in mitosis. *Cell Signal* **19**, 1964-1972 (2007).

24. Pereira, D.M. & Rodrigues, C.M.P. Targeted Avenues for Cancer Treatment: The MEK5-ERK5 Signaling Pathway. *Trends Mol Med* **26**, 394-407 (2020).

25. Aza-Blanc, P. *et al.* Identification of modulators of TRAIL-induced apoptosis via RNAi-based phenotypic screening. *Mol Cell* **12**, 627-637 (2003).

26. Borges, J., Pandiella, A. & Esparis-Ogando, A. Erk5 nuclear location is independent on dual phosphorylation, and favours resistance to TRAIL-induced apoptosis. *Cell Signal* **19**, 1473-1487 (2007).

27. Lane, D., Goncharenko-Khaider, N., Rancourt, C. & Piche, A. Ovarian cancer ascites protects from TRAIL-induced cell death through alphavbeta5 integrin-mediated focal adhesion kinase and Akt activation. *Oncogene* **29**, 3519-3531 (2010).

bioRxiv preprint doi: https://doi.org/10.1101/2023.03.22.533738; this version posted March 24, 2023. The copyright holder for this preprint (which was not certified by peer review) is the author/funder, who has granted bioRxiv a license to display the preprint in perpetuity. It is made available under aCC-BY-NC-ND 4.0 International license.

28. Pallares, J. *et al.* Abnormalities in the NF-kappaB family and related proteins in endometrial carcinoma. *J Pathol* **204**, 569-577 (2004).

29. Wang, J. *et al.* Structural and Atropisomeric Factors Governing the Selectivity of Pyrimido-benzodiazipinones as Inhibitors of Kinases and Bromodomains. *ACS Chem.Biol.* **13**, 2438-2448 (2018).

30. Lin, E.C. *et al.* ERK5 kinase activity is dispensable for cellular immune response and proliferation. *Proc Natl Acad Sci U S A* **113**, 11865-11870 (2016).

31. Tatake, R.J. *et al.* Identification of pharmacological inhibitors of the MEK5/ERK5 pathway. *Biochem Biophys Res Commun* **377**, 120-125 (2008).

32. Gatsinzi, T., Ivanova, E.V. & Iverfeldt, K. TRAIL resistance in human neuroblastoma SK-N-AS cells is dependent on protein kinase C and involves inhibition of caspase-3 proteolytic processing. *J Neurooncol* **109**, 503-512 (2012).

33. Poondla, N., Chandrasekaran, A.P., Heese, K., Kim, K.S. & Ramakrishna, S. CRISPR-mediated upregulation of DR5 and downregulation of cFLIP synergistically sensitize HeLa cells to TRAIL-mediated apoptosis. *Biochem Biophys Res Commun* **512**, 60-65 (2019).

34. Reis, C.R., Chen, P.H., Bendris, N. & Schmid, S.L. TRAIL-death receptor endocytosis and apoptosis are selectively regulated by dynamin-1 activation. *Proc Natl Acad Sci U S A* **114**, 504-509 (2017).

35. Chen, X. *et al.* Constitutively active Akt is an important regulator of TRAIL sensitivity in prostate cancer. *Oncogene* **20**, 6073-6083 (2001).

36. Tummers, B. & Green, D.R. Caspase-8: regulating life and death. *Immunol Rev* **277**, 76-89 (2017).

37. Wang, X. *et al.* Targeted deletion of mek5 causes early embryonic death and defects in the extracellular signal-regulated kinase 5/myocyte enhancer factor 2 cell survival pathway. *Mol.Cell Biol.* **25**, 336-345 (2005).

38. Berg, H.F. *et al.* Patient-derived organoids reflect the genetic profile of endometrial tumors and predict patient prognosis. *Commun Med (Lond)* **1**, 20 (2021).

39. Villafranca-Magdalena, B. *et al.* Genomic Validation of Endometrial Cancer Patient-Derived Xenograft Models as a Preclinical Tool. *Int J Mol Sci* **23** (2022).

bioRxiv preprint doi: https://doi.org/10.1101/2023.03.22.533738; this version posted March 24, 2023. The copyright holder for this preprint (which was not certified by peer review) is the author/funder, who has granted bioRxiv a license to display the preprint in perpetuity. It is made available under aCC-BY-NC-ND 4.0 International license.

40. Mauvezin, C. *et al.* The nuclear cofactor DOR regulates autophagy in mammalian and Drosophila cells. *EMBO Rep* **11**, 37-44 (2010).

41. Sala, D. *et al.* Autophagy-regulating TP53INP2 mediates muscle wasting and is repressed in diabetes. *J Clin Invest* **124**, 1914-1927 (2014).

42. Brown, H.A. *et al.* An ERK5-KLF2 signalling module regulates early embryonic gene expression and telomere rejuvenation in stem cells. *Biochem J* **478**, 4119-4136 (2021).

43. Vaseva, A.V. *et al.* KRAS Suppression-Induced Degradation of MYC Is Antagonized by a MEK5-ERK5 Compensatory Mechanism. *Cancer Cell* **34**, 807-822 e807 (2018).

44. Erazo, T. *et al.* Canonical and kinase activity-independent mechanisms for extracellular signal-regulated kinase 5 (ERK5) nuclear translocation require dissociation of Hsp90 from the ERK5-Cdc37 complex. *Mol Cell Biol* **33**, 1671-1686 (2013).

45. Mody, N., Campbell, D.G., Morrice, N., Peggie, M. & Cohen, P. An analysis of the phosphorylation and activation of extracellular-signal-regulated protein kinase 5 (ERK5) by mitogen-activated protein kinase kinase 5 (MKK5) in vitro. *Biochem J* **372**, 567-575 (2003).

46. Prager, I. & Watzl, C. Mechanisms of natural killer cell-mediated cellular cytotoxicity. *J Leukoc Biol* **105**, 1319-1329 (2019).

47. Duan, S. *et al.* Natural killer group 2D receptor and its ligands in cancer immune escape. *Mol Cancer* **18**, 29 (2019).

48. Kataoka, T. *et al.* Concanamycin A, a powerful tool for characterization and estimation of contribution of perforin- and Fas-based lytic pathways in cell-mediated cytotoxicity. *J Immunol* **156**, 3678-3686 (1996).

49. Lemke, J., von Karstedt, S., Zinngrebe, J. & Walczak, H. Getting TRAIL back on track for cancer therapy. *Cell Death Differ* **21**, 1350-1364 (2014).

50. Alvarez-Fernandez, S. *et al.* Potent antimyeloma activity of a novel ERK5/CDK inhibitor. *Clin Cancer Res* **19**, 2677-2687 (2013).

51. Ogasawara, J. *et al.* Lethal effect of the anti-Fas antibody in mice. *Nature* **364**, 806-809 (1993).

52. Costelli, P. *et al.* Mice lacking TNFalpha receptors 1 and 2 are resistant to death and fulminant liver injury induced by agonistic anti-Fas antibody. *Cell Death Differ* **10**, 997-1004 (2003).

bioRxiv preprint doi: https://doi.org/10.1101/2023.03.22.533738; this version posted March 24, 2023. The copyright holder for this preprint (which was not certified by peer review) is the author/funder, who has granted bioRxiv a license to display the preprint in perpetuity. It is made available under aCC-BY-NC-ND 4.0 International license.

53. von Karstedt, S., Montinaro, A. & Walczak, H. Exploring the TRAILs less travelled: TRAIL in cancer biology and therapy. *Nat Rev Cancer* **17**, 352-366 (2017).

54. Cristofanon, S. & Fulda, S. ABT-737 promotes tBid mitochondrial accumulation to enhance TRAIL-induced apoptosis in glioblastoma cells. *Cell Death Dis* **3**, e432 (2012).

55. Pal, S., Amin, P.J., Sainis, K.B. & Shankar, B.S. Potential Role of TRAIL in Metastasis of Mutant KRAS Expressing Lung Adenocarcinoma. *Cancer Microenviron* **9**, 77-84 (2016).

56. Liu, S. *et al.* NK cell-based cancer immunotherapy: from basic biology to clinical development. *J Hematol Oncol* **14**, 7 (2021).

57. Sordo-Bahamonde, C., Lorenzo-Herrero, S., Payer, A.R., Gonzalez, S. & Lopez-Soto, A. Mechanisms of Apoptosis Resistance to NK Cell-Mediated Cytotoxicity in Cancer. *Int J Mol Sci* **21** (2020).

58. Charni, S. *et al.* ERK5 knockdown generates mouse leukemia cells with low MHC class I levels that activate NK cells and block tumorigenesis. *J Immunol* **182**, 3398-3405 (2009).

59. Lopez-Botet, M., De Maria, A., Muntasell, A., Della Chiesa, M. & Vilches, C. Adaptive NK cell response to human cytomegalovirus: Facts and open issues. *Semin Immunol* **65**, 101706 (2023).

60. Pereira, D.M. *et al.* MEK5/ERK5 signaling inhibition increases colon cancer cell sensitivity to 5-fluorouracil through a p53-dependent mechanism. *Oncotarget* **7**, 34322-34340 (2016).

61. Shukla, A. *et al.* Extracellular signal-regulated kinase 5: a potential therapeutic target for malignant mesotheliomas. *Clin.Cancer Res.* **19**, 2071-2083 (2013).

62. Yang, Q. *et al.* BMK1 is involved in the regulation of p53 through disrupting the PML-MDM2 interaction. *Oncogene* (2012).

63. Kondoh, K., Terasawa, K., Morimoto, H. & Nishida, E. Regulation of nuclear translocation of extracellular signal-regulated kinase 5 by active nuclear import and export mechanisms. *Mol.Cell Biol.* **26**, 1679-1690 (2006).

64. Schimmel, J. *et al.* The ubiquitin-proteasome system is a key component of the SUMO-2/3 cycle. *Mol Cell Proteomics* **7**, 2107-2122 (2008).

65. Gamez-Garcia, A. *et al.* ERK5 Inhibition Induces Autophagy-Mediated Cancer Cell Death by Activating ER Stress. *Front Cell Dev Biol* **9**, 742049 (2021).

bioRxiv preprint doi: https://doi.org/10.1101/2023.03.22.533738; this version posted March 24, 2023. The copyright holder for this preprint (which was not certified by peer review) is the author/funder, who has granted bioRxiv a license to display the preprint in perpetuity. It is made available under aCC-BY-NC-ND 4.0 International license.

Figure legends

Figure 1. ERK5 inhibition sensitizes cancer cells to DR ligands-induced apoptosis by favoring Caspase-8 activation. A, ERK5 inhibition sensitizes EC cells to TRAIL-induced cytotoxicity. EC cells were pre-incubated with ERK5i JWG-071 for 12 h, previous treatment with TRAIL for 24 h (mean ± SD, n = 4 independent biological experiments, one-way ANOVA). Lower tables show cell viabilities (%) of each pairwise combination of drug doses (blue color, maximum cell viability; red color, minimum cell viability). **B,** Inhibitors of the MEK5-ERK5 pathway sensitize Ishikawa EC cells to TRAIL-induced cytotoxicity. EC cells were pre-incubated with different ERK5i (JWG-071 and AX-15836) or MEK5i (BIX02188 and BIX02189) for 12 h, previous treatment with TRAIL for 24 h (mean ± SD, n = 3 independent biological experiments, one-way ANOVA). **C**. ERK5 inhibition sensitizes EC cells to TNF-α and anti-Fas activating antibody. EC cells were pre-incubated with ERK5i JWG-071 for 12 h, previous treatment with TNF-α or anti-Fas for 24 h (mean ± SD, n = 4 independent biological experiments, one-way ANOVA). Lower tables show cell viabilities (%) of each pairwise combination of drug doses (blue color, maximum cell viability; red color, minimum cell viability). **D,** ERK5 inhibition sensitizes different human cancer cell lines to TRAIL-induced cytotoxicity. Cell viability experiments were performed as in **A**. **E,** ERK5 inhibition enhances caspase-8 activation induced by DR ligands. Ishikawa cells pre-treated with 5 μM JWG-071 (12 h) were treated (4 h) with TRAIL, TNFα or anti-Fas activating antibody. Caspase-8 and Caspase-3 activation was monitored by immunoblot analysis. **F,** Inhibition of caspases prevents sensitization to TRAIL induced by ERK5i. Ishikawa cells pre-treated (2 h) with pan-caspase inhibitor Q-VD-OPH were treated with 5 μM JWG-071 (12 h) and further exposed to 100 ng/ml TRAIL for 24h. Histograms show the % of cell viability. Statistical significance was calculated using one-way ANOVA followed by Bonferroni multiple comparison test. Unless indicated, p-values refer to statistical difference of combined (TRAIL and ERK5i) vs TRAIL single treatment.

Figure 2. ERK5 kinase activity confers resistance to TRAIL-induced apoptosis in cancer cells. A, Active ERK5 protects AN3CA EC cells to TRAIL-induced apoptosis. AN3CA EC cells were transfected with either ERK5 or a ERK5 kinase-dead mutant (D200A, ERK5-KD) together with a constitutively active form of MEK5 (MEK5-DD). Twenty-four hours after transfection cells were treated with 25 ng/ml TRAIL (8 h), and apoptosis was analyzed by flow cytometry (Annexin-V and PI staining). Left panel shows representative results of flow cytometry analysis. Right histograms show the quantification of apoptotic cells (early apoptotic Annexin-V+/PI- and late apoptotic Annexin-V+/PI+ cells). **B-C,** ERK5 kinase

bioRxiv preprint doi: https://doi.org/10.1101/2023.03.22.533738; this version posted March 24, 2023. The copyright holder for this preprint (which was not certified by peer review) is the author/funder, who has granted bioRxiv a license to display the preprint in perpetuity. It is made available under aCC-BY-NC-ND 4.0 International license.

activity impairs caspase-8 activation in response to TRAIL in AN3Ca (B) and Ishikawa (C) cells. Immunoblot analysis. Right histograms show the quantification of cleaved caspase-8 and -3 bands (mean ± SD, n = 3 independent biological experiments, one-way ANOVA followed by Bonferroni multiple comparison test). ***p < 0.001.

Figure 3. ERK5 or MEK5 genetic deletion sensitizes Ishikawa EC cells to DR agonists-induced apoptosis by favoring Caspase-8 activation. A, Ishikawa wild type, MEK5-KO or ERK5-KO cells were treated for 24 h with 50 ng/ml TRAIL, 20 ng/ml TNFα or 100 ng/ml Anti-Fas activating antibody, and apoptotic cells were analyzed by flow cytometry (Annexin-V and PI staining). Right histograms show the quantification of apoptotic cells (mean ± SD, n =3 independent biological experiments, one-way ANOVA). **B-C,** MEK5 or ERK5 genetic deletion enhances caspase-8 activation in response to DR ligands. Ishikawa wild type, ERK5-KO (**B**) or MEK5-KO (**C**) cells were treated for 4 h with 50 ng/ml TRAIL, 20 ng/ml TNFα or 100 ng/ml Anti-Fas activating antibody. Caspase-8 and caspase-3 activation was monitored by immunoblot analysis. **D,** MEK5 genetic deletion sensitizes 3D cultures of Ishikawa cells to DR ligands. 3D cultures were treated with 50 ng/ml TRAIL, 20 ng/ml TNFα or 100 ng/ml Anti-Fas activating antibody for 24 h, and cell viability was analyzed with LIVE/DEAD reagent (alive cells, green; dead cells, red). **B-C,** similar results were obtained in three independent experiments.

Figure 4. ERK5 inhibition sensitizes PDX-derived organoids (PDX-Os) from endometroid cancer patients to TRAIL-induced cytotoxicity. A-B, PDX-Os recapitulates the morphological organization of endometrial tumors. Confocal immunofluorescence imaging of PDX-Os from patients 440 and 1297 stained with epithelial (EpCAM and E-cadherin), mesenchymal (vimentin), cytoskeleton (F-actin) and nuclei (DAPI) markers. Scale bars are represented in the bright field photos. **C-D,** ERK5 inhibition sensitize EC PDX-Os to TRAIL-induced cytotoxicity. PDX-Os from patients 440 and 1297 were pre-treated with either vehicle or 5 μM JWG-071 for 12 h, previous treatment with TRAIL (48 h). Cytotoxicity was assessed by measuring intracellular ATP levels in PDXOs (**C**), or by LIVE/DEAD staining of PDX-Os (**D**) (alive cells, green; dead cells, red). Statistical significance was calculated using one-way ANOVA followed by Bonferroni multiple comparison test. Individual p-values are indicated in each figure.

Figure 5. ERK5 inhibition or genetic deletion sensitize cancer cells to DR agonists by increasing TP53INP2 protein levels. A, ERK5 inhibition upregulates TP53INP2 protein levels in EC cancer cells. Ishikawa, ARK1, ARK2 and AN3CA EC cells were treated for 24 h with either vehicle or 5 μM JWG-071. TP53INP2 and DR5 protein levels were determined by immunoblot analysis. **B,** ERK5 or MEK5 genetic

bioRxiv preprint doi: https://doi.org/10.1101/2023.03.22.533738; this version posted March 24, 2023. The copyright holder for this preprint (which was not certified by peer review) is the author/funder, who has granted bioRxiv a license to display the preprint in perpetuity. It is made available under aCC-BY-NC-ND 4.0 International license.

deletion upregulates TP53INP2 protein levels. **C,** ERK5 inhibition increases the amount of TP53INP2 bound to Caspase-8. HEK293T cells overexpressing FLAG-TP53INP2 were treated with either vehicle or 3 μM JWG-071 for 6 h. After immunoprecipitation of FLAG-TP53INP2, the presence of Caspase-8 in the immunoprecipitated fraction was detected by immunoblot analysis. **D**. TP53INP2 mediates the sensitization of EC cells to DR agonists exerted by ERK5i. Ishikawa wild type TP53INP2-KO cells were pre-treated 3 μM JWG-071 (16 h), treated with 50 ng/ml TRAIL, 20 ng/ml TNFα or 100 ng/ml Anti-Fas activating antibody for 24 h, and apoptotic cells were analyzed by flow cytometry (Annexin-V and PI staining). Lower panel shows the corresponding quantification of the results of three independent biological experiments (one-way ANOVA followed by Bonferroni multiple comparison test). **E-F,** ERK5 inhibition favors caspase-8 activation in response to DR-ligands in a TP53INP2 protein-dependent manner. Caspase-8 activation was measured by a luminescent substrate (LETD) assay (**E**), or by monitoring Caspase-8 cleavage by immunoblot (**F**). Cells were pre-treated with JWG-071 (12 h) and further treated with 50 ng/ml TRAIL, 20 ng/ml TNFα or 100 ng/ml Anti-Fas activating antibody for 4 h. **G-H,** ERK5 inhibition sensitize 3D cultures of EC Ishikawa cells to TRAIL in a TP53INP2-dependent manner. 3D cultures of Ishikawa wild type or TP53INP2-KO cells were pre-treated 12h with JWG-071, and further treated with the indicated concentrations of TRAIL for 24 h. Viability of the 3D cultures was assessed by measuring intracellular ATP-content (**G**) or by LIVE/DEAD staining (**H**). Alive (green) and dead cells (red) were visualized by fluorescence microscopy. Statistical significance of **E** and **G** was calculated using one-way ANOVA followed by Bonferroni multiple comparison test. Individual p-values are indicated in each panel.

Figure 6. ERK5 phosphorylation of TP53INP2 induces ubiquitylation and proteasomal degradation of TP53INP2. **A**, Active ERK5 overexpression induces TP53INP2 proteasomal degradation. HEK293T were transfected with vectors encoding for FLAG-TP53INP2 and GST-tagged wild type ERK5 (ERK5-WT) or ERK5 kinase-dead mutant (ERK5-KD), in combination with a vector encoding for a constitutively active form of MEK5 (MEK5-DD). Cells were treated with either vehicle or MG-132 (4 h), and protein levels monitored by immunoblot analysis. **B**. ERK5 kinase activity induces TP53INP2 ubiquitylation. HEK293T cells were transfected with plasmids encoding for FLAG-TP53INP2 and His-tagged ubiquitin, and/or for GST-tagged ERK5 and MEK5DD (active ERK5). After incubating with MG-132 (4 h), ubiquitylated TP53INP2 was affinity-purified and detected by immunoblotting. **C,** Active ERK5 does not induce proteasomal degradation of the ubiquitin-deficient mutant TP53INP2-

bioRxiv preprint doi: https://doi.org/10.1101/2023.03.22.533738; this version posted March 24, 2023. The copyright holder for this preprint (which was not certified by peer review) is the author/funder, who has granted bioRxiv a license to display the preprint in perpetuity. It is made available under aCC-BY-NC-ND 4.0 International license.

3K/R. Experiment was performed as in **A**. **D,** ERK5 inhibition stabilizes TP53INP2 protein levels. Immunoblot analysis of HEK293 cell lysates overexpressing wild type or ubiquitin-deficient mutant, treated with ERK5i and the protein synthesis inhibitor cyclohexamide (CHX) for 8 hours. **E,** ERK5 interacts with TP53INP2. One milligram of Ishikawa cell lysates was immunoprecipitated with anti-ERK5 antibody, and levels of pelleted TP53INP2 and ERK5 were monitored by immunoblot analysis. **F-G**, ERK5 phosphorylates TP53INP2 at Ser49, Ser65 and Thr74. **F,** FLAG-TP53INP2 protein expressed in HEK293T was affinity purified, and incubated with pure active ERK5 in the presence of [γ-^{32}P]-ATP. After resolving the proteins by SDS/PAGE electrophoresis, incorporation of ^{32}P was monitored by autoradiography. **G,** Schematic representation of the TP53INP2-3A phospho-deficient mutant. **H,** The TP53INP2-3A mutant is poorly phosphorylated by ERK5. Experiment was performed as in **F**. **I,** The TP53INP2 mutants TP53INP2-3A and TP53INP2-3K/R have higher protein expression than wild-type TP53INP2, and ERK5i does not affect protein levels of TP53INP2-3A and TP53INP2-3K/R mutants. Immunoblot analysis. **J-K**, ERK5 phosphorylation induces TP53INP2 ubiquitylation and proteasomal degradation. **J**, Denaturing ubiquitylation assay of HEK293T cell lysates. Experiment was performed as described in **B**. **K,** Immunoblot analysis of cells expressing wild-type, 3A or 3K/R mutants of TP53INP2, after blocking protein synthesis with cyclohexamide for the indicated times. Right panel shows the quantification of three independent experiments, and the half-life values for each of the TP53INP2 mutants.

Figure 7. ERK5 inhibition does not alter apoptotic transcriptional programs in Ishikawa EC cells. **A.** Volcano plot of RNAseq expression data after ERK5 inhibition in EC Ishikawa cells. The plot shows the upregulated (in red) and downregulated (in blue) differentially expressed genes (DEGs) (Qvalue < 0.05, $\log_2$ fold change >|1.5|). Source data is provided as a Supplementary Data file. **B,** ERK5 kinase activity positively regulates gene transcription in EC cells. Heatmap of the 260 DEGs (Qvalue < 0.05, $\log_2$ fold change >|1.5|) in response to ERK5 inhibition. **C,** Top-5 upregulated and top-5 downregulated hallmark genesets in response to ERK5 inhibition. **D-E-F** Gene set enrichment analysis (GSEA) of Hallmark_apoptosis (**D**), or GOBP-extrinsic apoptotic signaling pathway **(E**) or GOBP-regulation of extrinsic apoptotic signaling pathway (**F**), in response to ERK5 inhibition. Lower panels show the corresponding heatmaps of the DEGs (Q value < 0.05, $\log_2$ fold change >|1|).

Figure 8. ERK5 inhibition or genetic deletion sensitizes Ishikawa EC cells to the cytotoxicity induced by the TRAIL and FasL expressed by eNK cells. **A-B,** Expanded NK cells express

bioRxiv preprint doi: https://doi.org/10.1101/2023.03.22.533738; this version posted March 24, 2023. The copyright holder for this preprint (which was not certified by peer review) is the author/funder, who has granted bioRxiv a license to display the preprint in perpetuity. It is made available under aCC-BY-NC-ND 4.0 International license.

detectable TRAIL and FasL proteins at the membrane**. A,** TRAIL expression at the membrane of eNKs was detected by flow cytometry analysis. **B,** eNK cells were co-cultured with Ishikawa EC cells (4 h) and surface FasL was detected by flow cytometry. **C,** Schematic representation of the experiments performed co-culturing eNKs and EC cancer cells. eNKs from four different healthy donors were treated for 2 h with either vehicle (DMSO) or concanamycin A (yellow shading) to inhibit Perforin. Concanamycin A was maintained during the co-culture. **D,** ERK5i enhances caspase-8 activation induced by eNKs (white shading), and caspase-8 activation induced by the eNKs TRAIL/FasL pathway (yellow shading) in EC cells. **E**, TP53INP2 mediates EC cell sensitization to eNKs TRAIL/FasL pathway exerted by ERK5i. Active caspase-3 flow cytometry assay. Yellow shading histograms: TP53INP2-KO Ishikawa EC cells show impaired activation of caspase-3 in response to the eNK TRAIL/FasL cytotoxic pathway. Results are the mean ± SD of four independent biological samples (donors). **F,** MEK5 or ERK5 genetic deletion sensitize Ishikawa EC cells to the cytotoxicity induced by the eNK TRAIL/FasL cytotoxic pathway. Flow cytometry analysis for caspase-3 activation (cleaved caspase-3). Right histograms show the corresponding caspase-3 quantification. Yellow shading histograms show the results obtained for the eNK TRAIL/FasL cytotoxic pathway. Results are the mean ± SD of four independent biological samples (donors). **D, E and F,** Statistical significance was calculated using one-way ANOVA followed by Bonferroni multiple comparison test. Individual p-values are indicated in each panel.

Figure 9. Schematic representation of the proposed mechanism for the role of the ERK5-TP53INP2 pathway in the sensitization of cancer cells to DR agonists-induced extrinsic apoptosis.

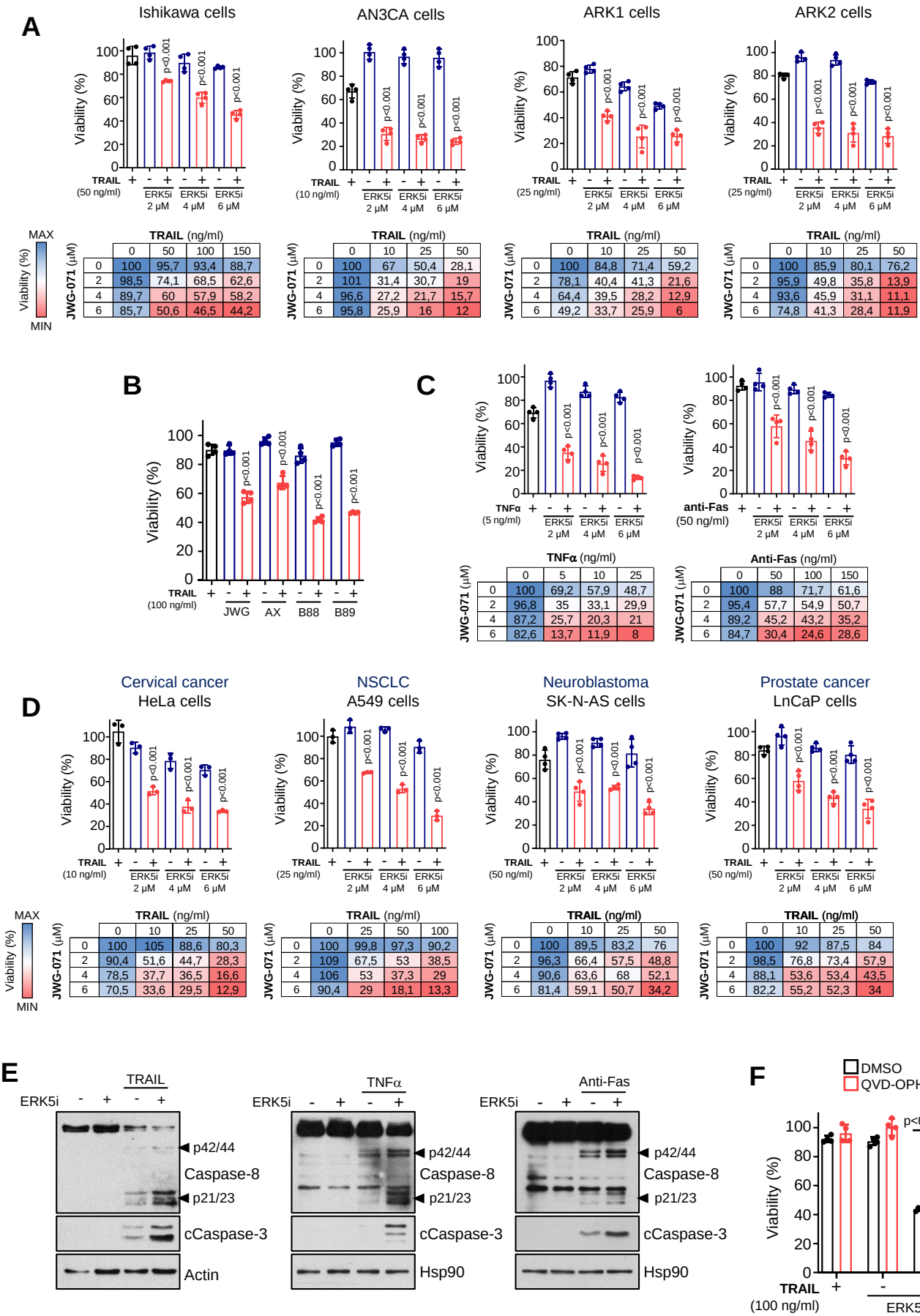
A
Ishikawa cells
AN3CA cells
ARK1 cells
ARK2 cells
Viability (%)
TRAIL
(50 ng/ml)
(10 ng/ml)
(25 ng/ml)
ERK5i
2 μM
4 μM
6 μM
p<0.001
MAX
MIN
JWG-071 (μM)
TRAIL (ng/ml)
0 100 95,7 93,4 88,7
2 98,5 74,1 68,5 62,6
4 89,7 60 57,9 58,2
6 85,7 50,6 46,5 44,2
0 100 67 50,4 28,1
2 101 31,4 30,7 19
4 96,6 27,2 21,7 15,7
6 95,8 25,9 16 12
0 100 84,8 71,4 59,2
2 78,1 40,4 41,3 21,6
4 64,4 39,5 28,2 12,9
6 49,2 33,7 25,9 6
0 100 85,9 80,1 76,2
2 95,9 49,8 35,8 13,9
4 93,6 45,9 31,1 11,1
6 74,8 41,3 28,4 11,9
B
JWG
AX
B88
B89
C
TNFα
(5 ng/ml)
anti-Fas
(50 ng/ml)
TNFα (ng/ml)
0 100 69,2 57,9 48,7
2 96,8 35 33,1 29,9
4 87,2 25,7 20,3 21
6 82,6 13,7 11,9 8
Anti-Fas (ng/ml)
0 100 88 71,7 61,6
2 95,4 57,7 54,9 50,7
4 89,2 45,2 43,2 35,2
6 84,7 30,4 24,6 28,6
D
Cervical cancer
HeLa cells
NSCLC
A549 cells
Neuroblastoma
SK-N-AS cells
Prostate cancer
LnCaP cells
0 100 105 88,6 80,3
2 90,4 51,6 44,7 28,3
4 78,5 37,7 36,5 16,6
6 70,5 33,6 29,5 12,9
0 100 99,8 97,3 90,2
2 109 67,5 53 38,5
4 106 53 37,3 29
6 90,4 29 18,1 13,3
0 100 89,5 83,2 76
2 96,3 66,4 57,5 48,8
4 90,6 63,6 68 52,1
6 81,4 59,1 50,7 34,2
0 100 92 87,5 84
2 98,5 76,8 73,4 57,9
4 88,1 53,6 53,4 43,5
6 82,2 55,2 52,3 34
E
TRAIL
TNFα
Anti-Fas
ERK5i
p42/44
Caspase-8
p21/23
cCaspase-3
Actin
Hsp90
F
DMSO
QVD-OPH
p<0.001
TRAIL
(100 ng/ml)
ERK5i

FIGURE 1

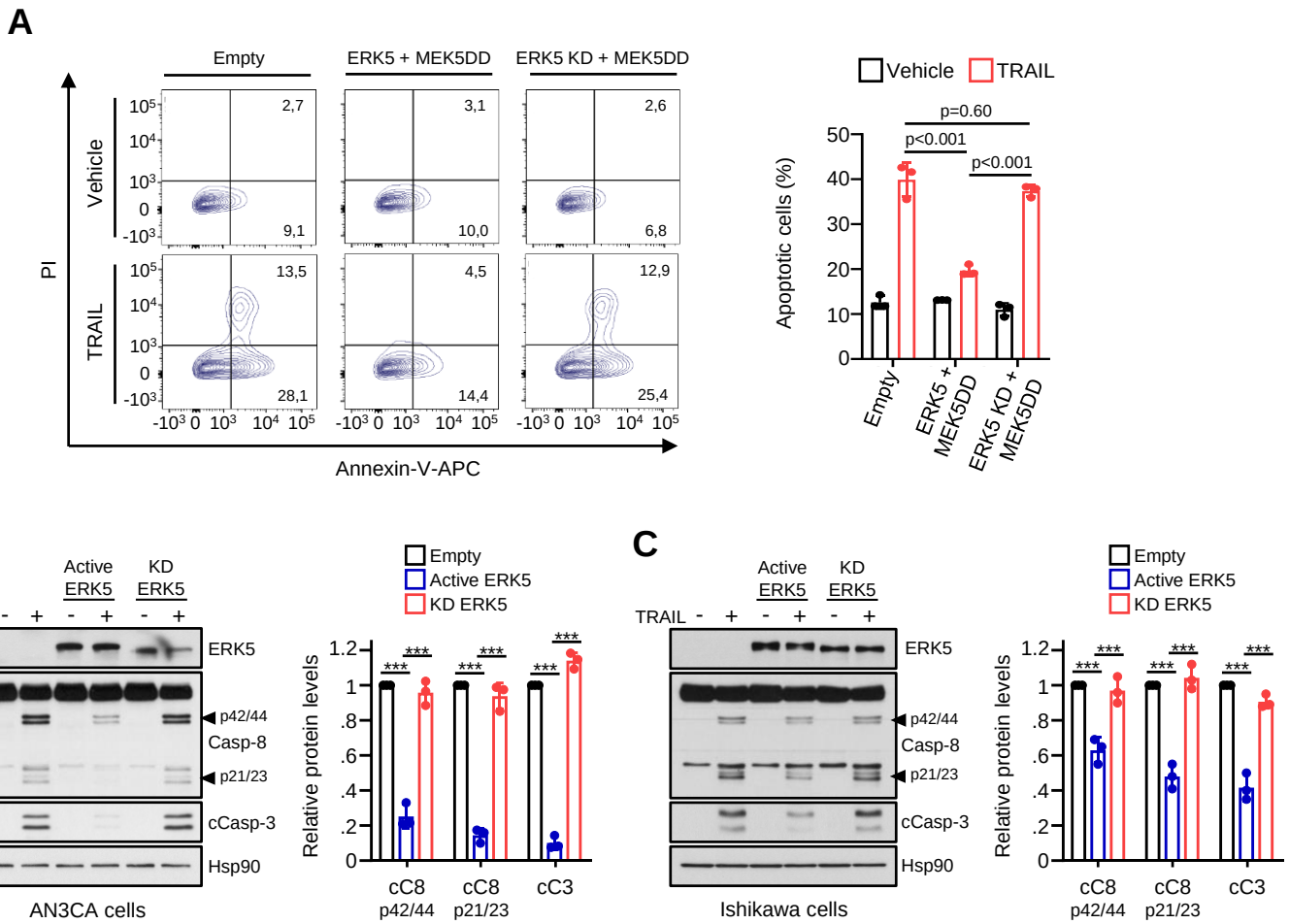
A
Empty
ERK5 + MEK5DD
ERK5 KD + MEK5DD
Vehicle
TRAIL
PI
Annexin-V-APC
2,7
9,1
3,1
10,0
2,6
6,8
13,5
28,1
4,5
14,4
12,9
25,4
Vehicle
TRAIL
Apoptotic cells (%)
p=0.60
p<0.001
p<0.001
Empty
ERK5 + MEK5DD
ERK5 KD + MEK5DD
B
Active ERK5
KD ERK5
TRAIL
ERK5
p42/44
Casp-8
p21/23
cCasp-3
Hsp90
AN3CA cells
Empty
Active ERK5
KD ERK5
Relative protein levels
cC8 p42/44
cC8 p21/23
cC3
C
Active ERK5
KD ERK5
TRAIL
ERK5
p42/44
Casp-8
p21/23
cCasp-3
Hsp90
Ishikawa cells
Empty
Active ERK5
KD ERK5
Relative protein levels
cC8 p42/44
cC8 p21/23
cC3

FIGURE 2

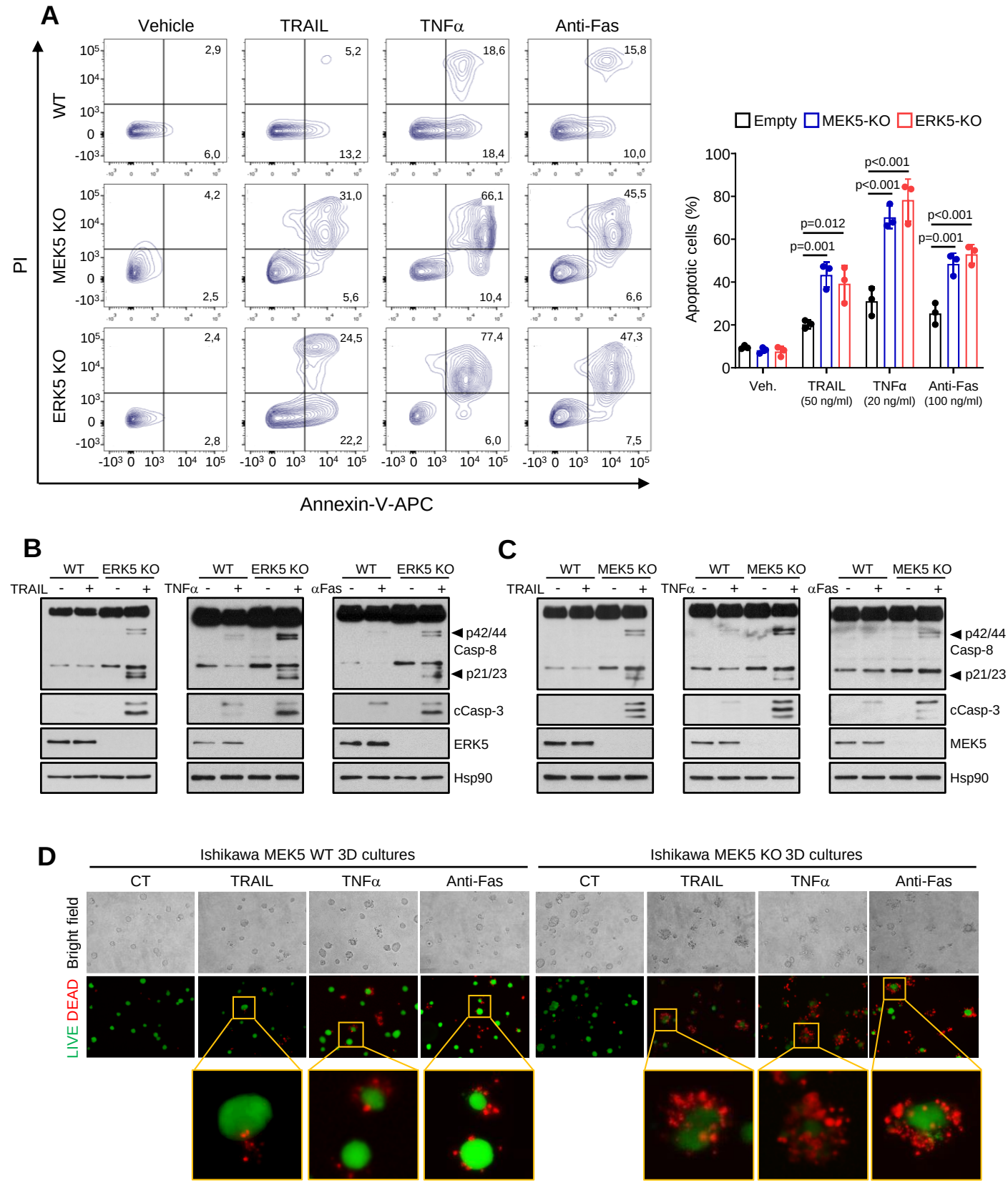
A
Vehicle
TRAIL
TNFα
Anti-Fas
WT
MEK5 KO
ERK5 KO
PI
Annexin-V-APC
2,9
6,0
5,2
13,2
18,6
18,4
15,8
10,0
4,2
2,5
31,0
5,6
66,1
10,4
45,5
6,6
2,4
2,8
24,5
22,2
77,4
6,0
47,3
7,5
Empty
MEK5-KO
ERK5-KO
Apoptotic cells (%)
p=0.001
p=0.012
p<0.001
p<0.001
p=0.001
p<0.001
Veh.
TRAIL (50 ng/ml)
TNFα (20 ng/ml)
Anti-Fas (100 ng/ml)
B
WT
ERK5 KO
TRAIL
TNFα
αFas
p42/44
Casp-8
p21/23
cCasp-3
ERK5
Hsp90
C
WT
MEK5 KO
TRAIL
TNFα
αFas
p42/44
Casp-8
p21/23
cCasp-3
MEK5
Hsp90
D
Ishikawa MEK5 WT 3D cultures
Ishikawa MEK5 KO 3D cultures
CT
TRAIL
TNFα
Anti-Fas
Bright field
LIVE DEAD

FIGURE 3

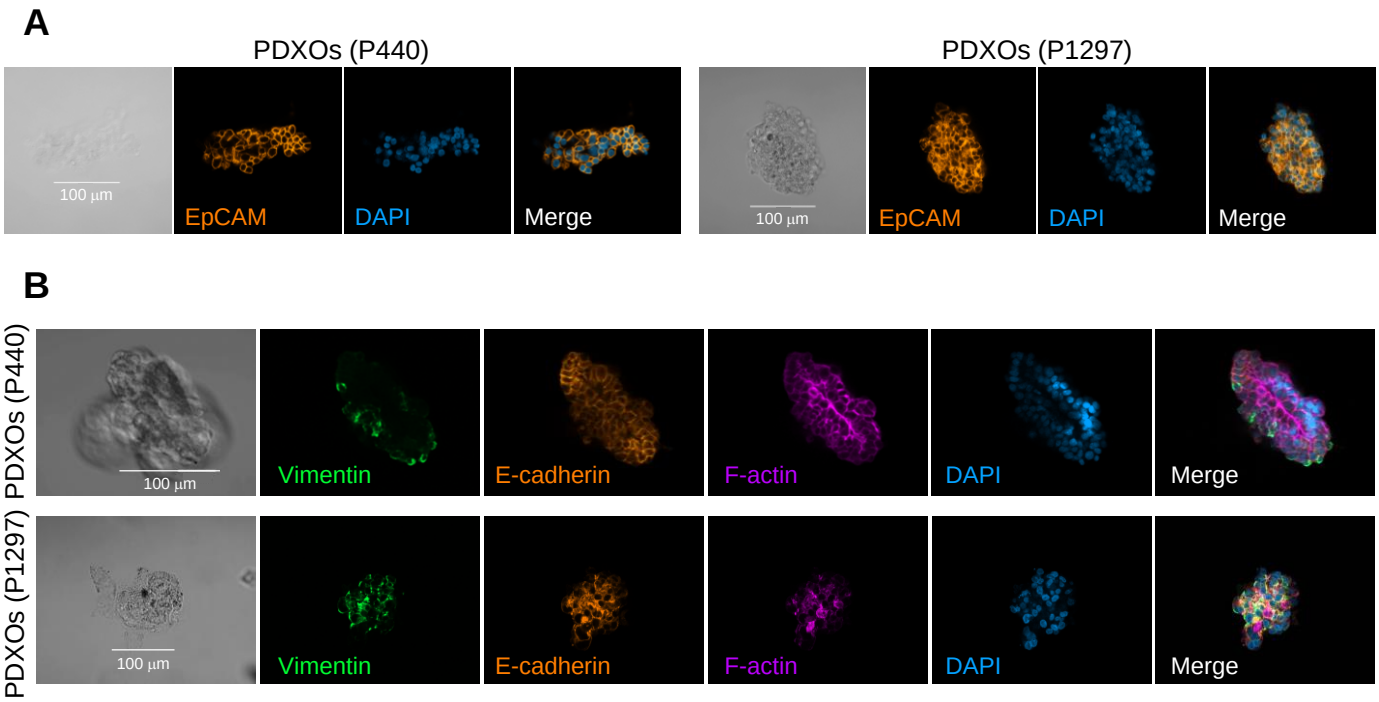
A
PDXOs (P440)
PDXOs (P1297)
100 µm
EpCAM
DAPI
Merge
B
PDXOs (P440)
PDXOs (P1297)
Vimentin
E-cadherin
F-actin
C
PDXOs (Patient 440)
Viability (%) (ATP content)
p<0.001
p<0.001
p<0.001
ERK5i
TRAIL
10
25
50 ng/ml
PDXOs (Patient 1297)
p=0.01
p<0.001
p<0.001
D
PDXOs (Patient 440)
CT
JWG-071
TRAIL
COMBO
Bright field
LIVE DEAD
PDXOs (Patient 1297)

FIGURE 4

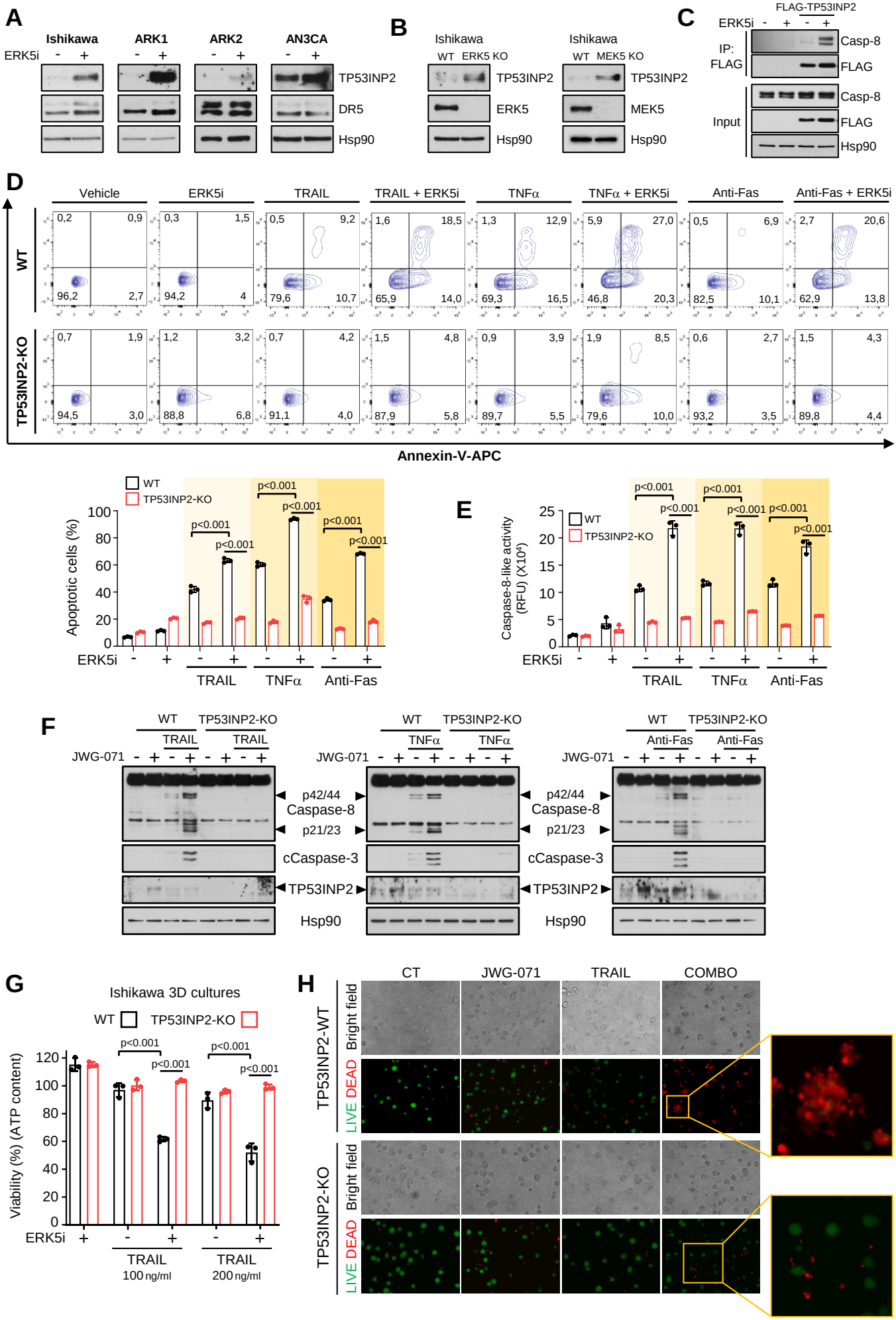
A
Ishikawa
ARK1
ARK2
AN3CA
ERK5i - + - + - + - +
TP53INP2
DR5
Hsp90
B
Ishikawa
WT ERK5 KO
TP53INP2
ERK5
Hsp90
Ishikawa
WT MEK5 KO
TP53INP2
MEK5
Hsp90
C
FLAG-TP53INP2
ERK5i - + - +
IP: FLAG
Casp-8
FLAG
Input
Casp-8
FLAG
Hsp90
D
Vehicle
ERK5i
TRAIL
TRAIL + ERK5i
TNFα
TNFα + ERK5i
Anti-Fas
Anti-Fas + ERK5i
WT
TP53INP2-KO
PI
Annexin-V-APC
0,2 0,9 96,2 2,7
0,3 1,5 94,2 4
0,5 9,2 79,6 10,7
1,6 18,5 65,9 14,0
1,3 12,9 69,3 16,5
5,9 27,0 46,8 20,3
0,5 6,9 82,5 10,1
2,7 20,6 62,9 13,8
0,7 1,9 94,5 3,0
1,2 3,2 88,8 6,8
0,7 4,2 91,1 4,0
1,5 4,8 87,9 5,8
0,9 3,9 89,7 5,5
1,9 8,5 79,6 10,0
0,6 2,7 93,2 3,5
1,5 4,3 89,8 4,4
WT
TP53INP2-KO
Apoptotic cells (%)
p<0.001
ERK5i - + - + - + - +
TRAIL
TNFα
Anti-Fas
E
Caspase-8-like activity (RFU) (X10⁴)
WT
TP53INP2-KO
p<0.001
ERK5i - + - + - + - +
TRAIL
TNFα
Anti-Fas
F
WT
TP53INP2-KO
TRAIL
TRAIL
JWG-071 - + - + - + - +
TNFα
TNFα
JWG-071 - + - + - + - +
Anti-Fas
Anti-Fas
JWG-071 - + - + - + - +
p42/44
Caspase-8
p21/23
cCaspase-3
TP53INP2
Hsp90
G
Ishikawa 3D cultures
WT
TP53INP2-KO
Viability (%) (ATP content)
p<0.001
ERK5i + - + - +
TRAIL 100 ng/ml
TRAIL 200 ng/ml
H
CT
JWG-071
TRAIL
COMBO
TP53INP2-WT
Bright field
LIVE DEAD
TP53INP2-KO
Bright field
LIVE DEAD

FIGURE 5

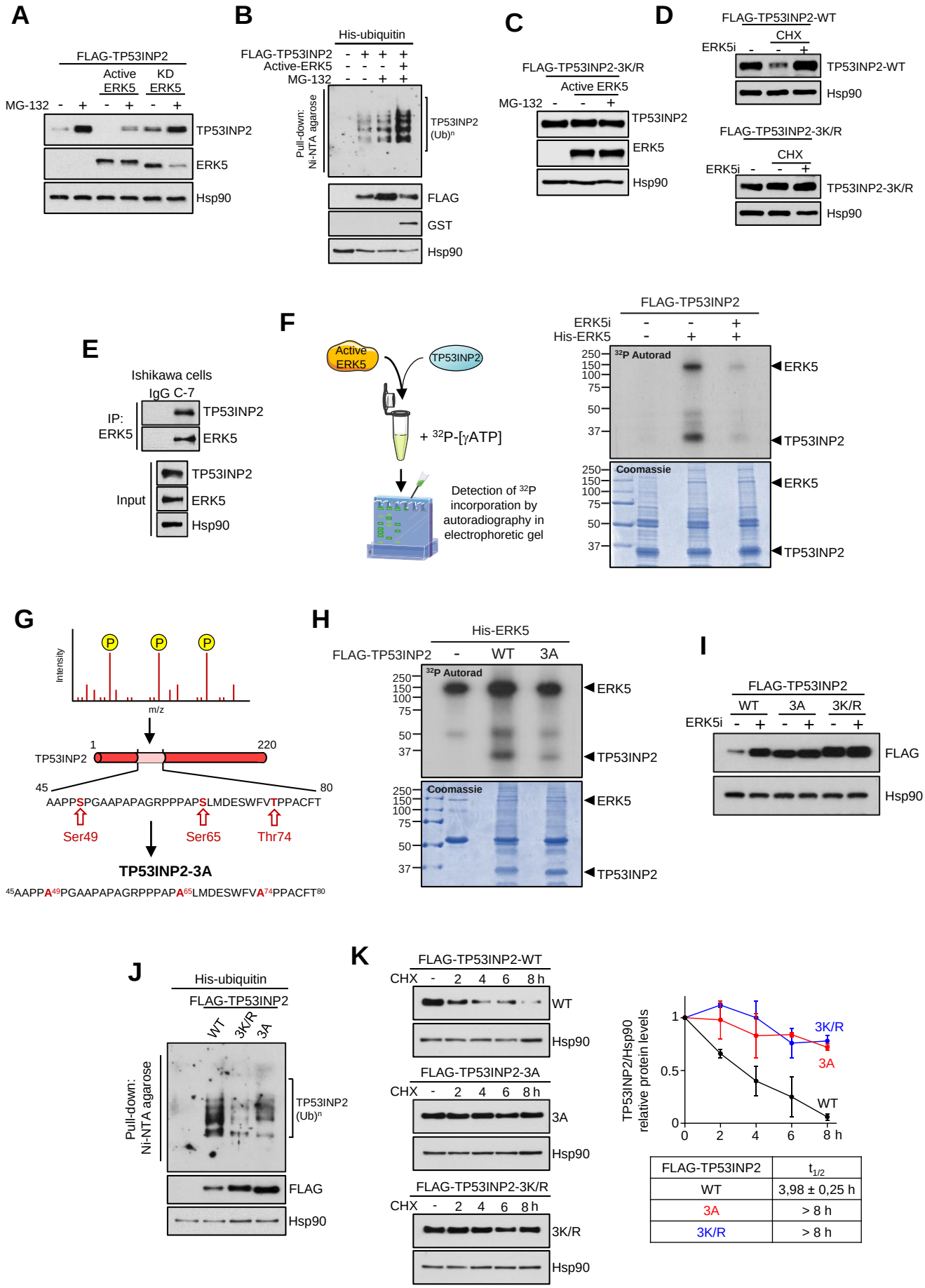

FLAG-TP53INP2	$t_{1/2}$
WT	3,98 ± 0,25 h
3A	> 8 h
3K/R	> 8 h

FIGURE 6

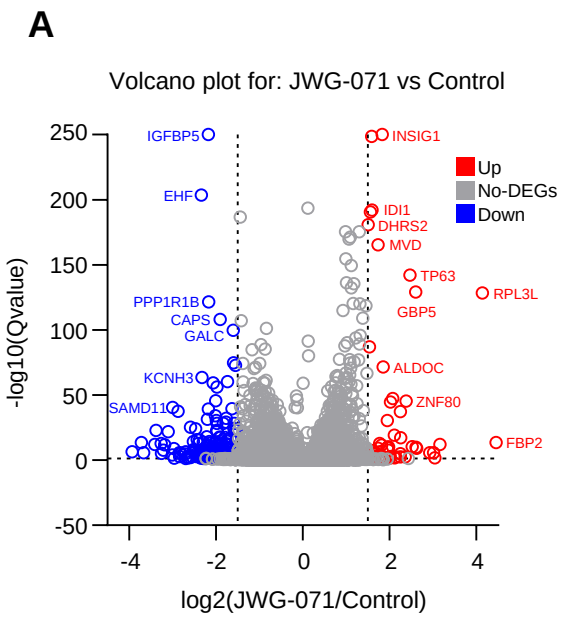

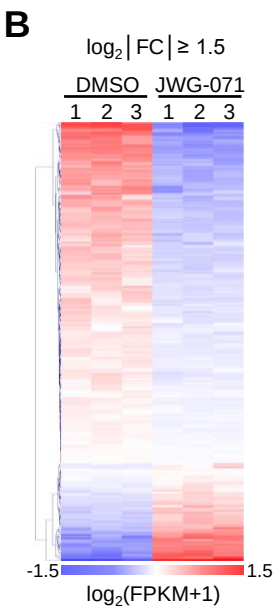

C

TOP 5 HALLMARK genesets downregulated in **JWG-071** condition

HALLMARK NAME	NES	FDR
ANGIOGENESIS	1.43	0.32
INTERFERON_ALPHA_RESPONSE	1.37	0.46
INTERFERON_GAMMA_RESPONSE	1.32	0.55
KRAS_SIGNALING_DN	1.27	0.66
ESTROGEN_RESPONSE_LATE	1.27	0.54

TOP 5 HALLMARK genesets upregulated in **JWG-071** condition

HALLMARK NAME	NES	FDR
PANCREAS_BETA_CELLS	-1.41	0.39
P53_PATHWAY	-1.38	0.34
CHOLESTEROL_HOMEOSTASIS	-1.33	0.33
MYC_TARGETS_V2	-1.30	0.32
MTORC1_SIGNALING	-1.29	0.28

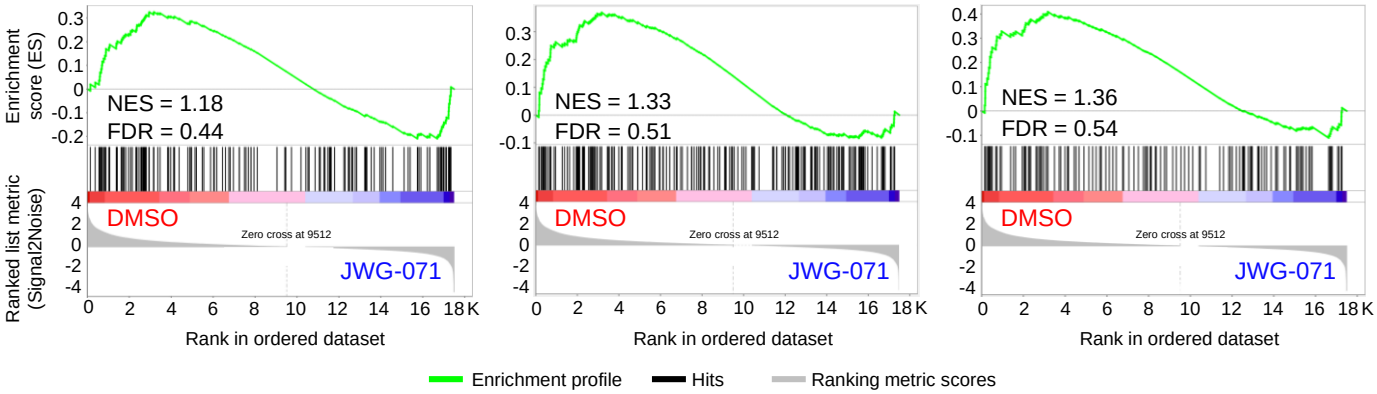

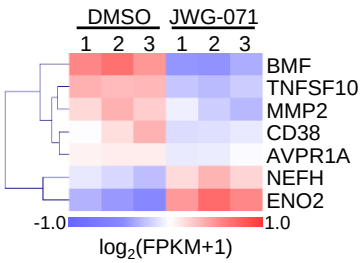

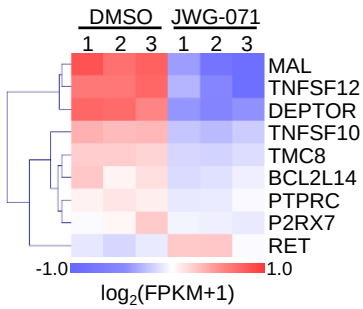

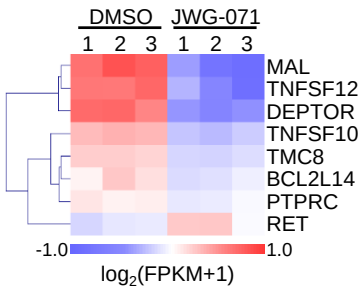

FIGURE 7

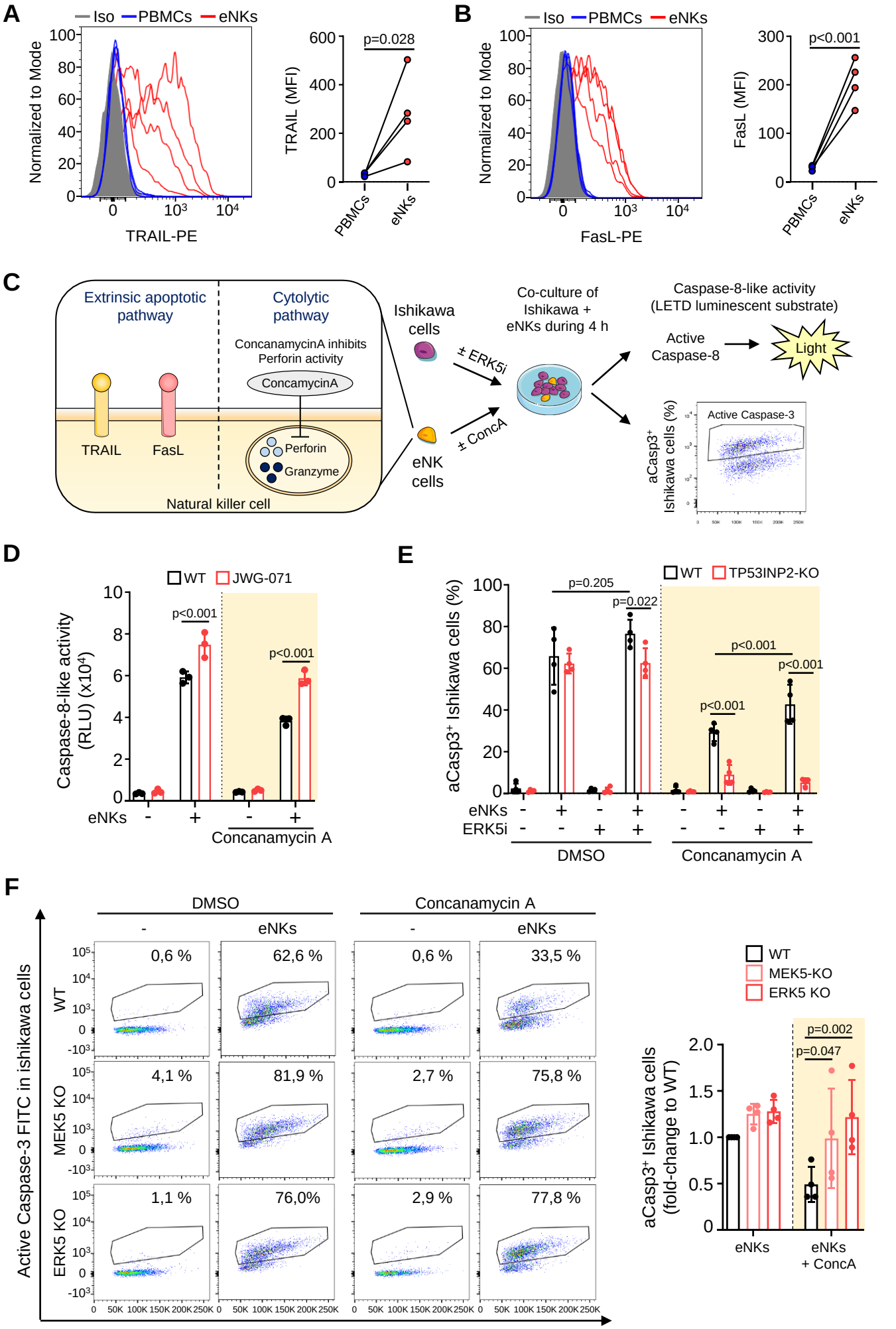
A
Iso
PBMCs
eNKs
Normalized to Mode
TRAIL-PE
TRAIL (MFI)
p=0.028
PBMCs
eNKs
B
FasL-PE
FasL (MFI)
p<0.001
C
Extrinsic apoptotic pathway
Cytolytic pathway
ConcanamycinA inhibits Perforin activity
ConcamycinA
TRAIL
FasL
Perforin
Granzyme
Natural killer cell
Ishikawa cells
eNK cells
± ERK5i
± ConcA
Co-culture of Ishikawa + eNKs during 4 h
Caspase-8-like activity (LETD luminescent substrate)
Active Caspase-8
Light
Active Caspase-3
aCasp3+ Ishikawa cells (%)
D
WT
JWG-071
Caspase-8-like activity (RLU) (x10⁴)
p<0.001
p<0.001
eNKs
Concanamycin A
E
WT
TP53INP2-KO
aCasp3+ Ishikawa cells (%)
p=0.205
p=0.022
p<0.001
p<0.001
p<0.001
p<0.001
eNKs
ERK5i
DMSO
Concanamycin A
F
DMSO
Concanamycin A
eNKs
WT
MEK5 KO
ERK5 KO
0,6 %
62,6 %
0,6 %
33,5 %
4,1 %
81,9 %
2,7 %
75,8 %
1,1 %
76,0%
2,9 %
77,8 %
Active Caspase-3 FITC in ishikawa cells
FSC-A
WT
MEK5-KO
ERK5 KO
aCasp3+ Ishikawa cells (fold-change to WT)
p=0.002
p=0.047
eNKs
eNKs + ConcA

FIGURE 8

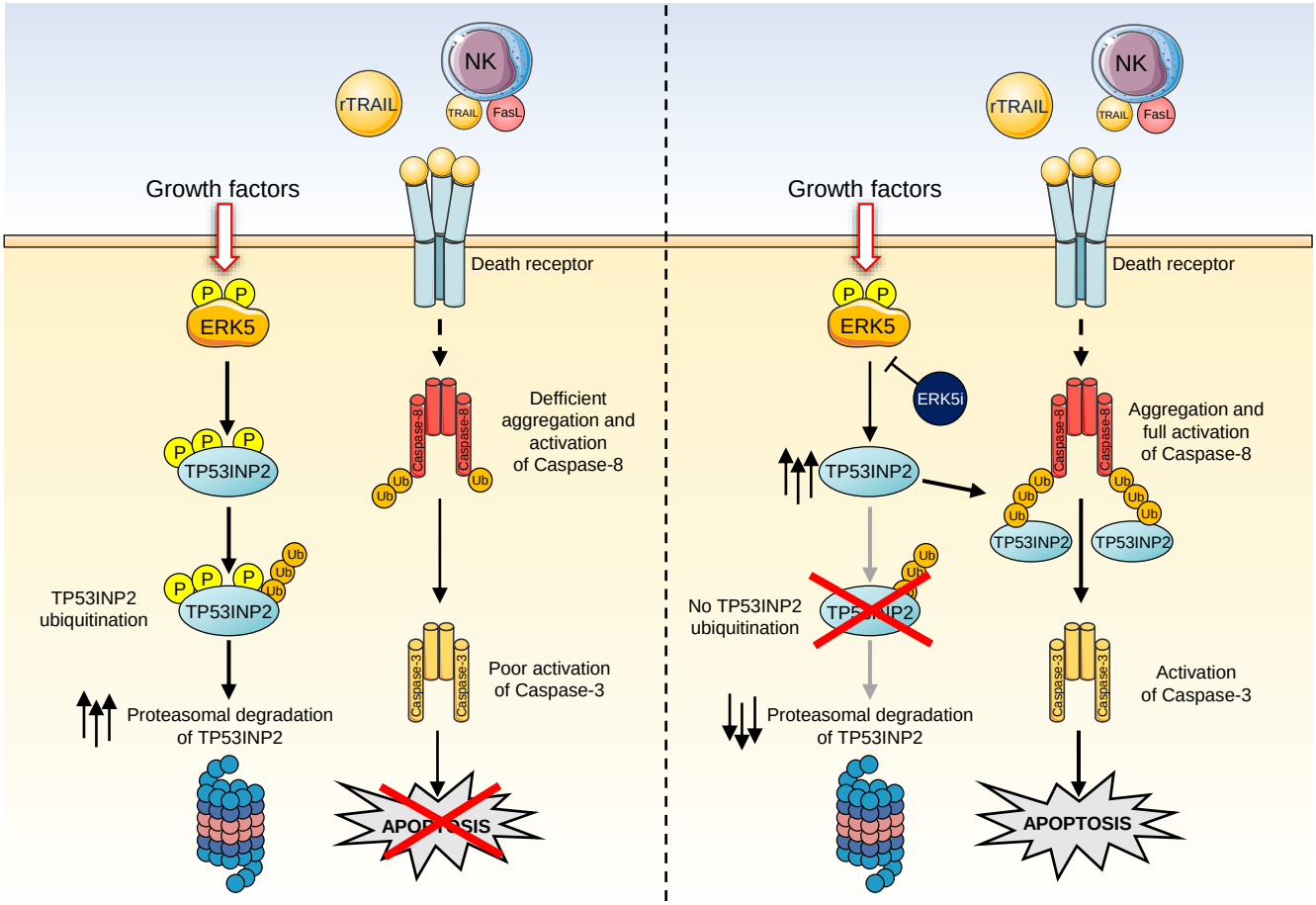
NK
rTRAIL
TRAIL
FasL
Growth factors
Death receptor
P
ERK5
TP53INP2
Ub
Caspase-8
Defficient aggregation and activation of Caspase-8
TP53INP2 ubiquitination
Proteasomal degradation of TP53INP2
Caspase-3
Poor activation of Caspase-3
APOPTOSIS
ERK5i
No TP53INP2 ubiquitination
Aggregation and full activation of Caspase-8
Activation of Caspase-3

FIGURE 9